The Nature of the Hydrophobic Binding of Small Peptides at the Bilayer Interface: Implications for the Insertion of Transbilayer Helices†

Russell E. Jacobs and Stephen H. White*

Department of Physiology and Biophysics, University of California, Irvine, Irvine, California 92717

Received January 27, 1988; Revised Manuscript Received December 7, 1988

ABSTRACT: One method of obtaining useful information about the physical chemistry of peptide/bilayer interactions is to relate thermodynamic parameters of the interactions to structural parameters obtained by diffraction methods. We report here the results of the application of this approach to interactions of hydrophobic tripeptides of the form Ala-X-Ala-*O-tert*-butyl with lipid bilayers. The thermodynamic constants (ΔG_t, ΔH_t, and ΔS_t) for the transfer of the tripeptides from water into DMPC vesicles were determined for X = Leu, Phe, and Trp and found to be consistent with those expected for hydrophobic interactions above the phase transition of DMPC. Combining these results with the earlier ones of Jacobs and White [(1986) *Biochemistry 25*, 2605–2612], the favorable free energies of transfer with different amino acids in the -X- position increase in the order Gly < Ala < Leu < Phe < Trp in agreement with the Nozaki and Tanford [(1971) *J. Biol. Chem. 246*, 2211–2217] hydrophobicity scale. Determination of the location of Ala-[$^2H_5$]Trp-Ala-*O-tert*-butyl in oriented DOPC bilayers by neutron diffraction shows that the most hydrophobic peptide of the series is confined to the bilayer headgroup/water region. Refinement of the diffraction measurements shows that only 13% of the tryptophan is associated with the hydrocarbon core. The distribution of the water tends to mirror that of the peptide. Unlike peptide-free bilayers, 5% of the water penetrates the hydrocarbon, which is about 100-fold greater than expected. A quantitative thermodynamic analysis of the interfacial binding of the peptides suggests that (1) the hydrophobic interactions are 60–70% complete upon binding at the bilayer interface, (2) the interface is likely to play an important role in helix formation and insertion, (3) the hydrogen bond status of amino acid side chains is crucial to insertion, and (4) an a priori lack of knowledge of the status of such bonds could limit the precision of hydrophobicity plots. We introduce an interfacial hydrophobicity scale, IFH(h), with a variable hydrogen bond parameter (h) that permits one to consider explicitly hydrogen bonding in transbilayer helix searches.

A major theme of membrane biochemistry is that membrane proteins form hydrophobic α-helices that span lipid bilayers. This idea, first proposed by Lenard and Singer (1966) and Wallach and Zahler (1966), became widely accepted with the demonstration of membrane-spanning proteins in erythrocytes (Bretcher, 1971), the determination of the low-resolution structure of bacteriorhodopsin, which apparently contains seven transmembrane helices (Henderson & Unwin, 1975), and the determination of the high-resolution structures of the photosynthetic reaction centers of *Rps.*[1] *viridis* (Deisenhofer et al., 1985) and *Rb. sphaeroides* (Allen et al., 1987), each of which contains eleven transmembrane helices. Considerable attention is now being given to so-called polarity (hydrophobicity) plot methods of predicting from primary structure the hydrophobic domains of membrane proteins which will presumably span the membrane bilayer as α-helices. Polarity plots are based upon fundamental assumptions about the thermodynamics of protein/bilayer interactions and are thus central to understanding the mechanisms of insertion of proteins into bilayers. These prediction methods (Von Heijne, 1981a,b; Engelman & Steitz, 1981, 1982; Kyte & Doolittle, 1982; Engelman et al., 1982) have been reviewed in detail by Eisenberg (1984) and by Engelman et al. (1986). They originate from the work of Rose and his colleagues who were concerned with the prediction of chain turns in globular proteins (Rose, 1978; Rose & Roy, 1980).

As discussed by Engelman et al. (1986), a major problem of polarity plots concerns the question of which polarity scale should be used for membrane proteins. The scales originate variously from experimental studies of the partitioning of amino acids between bulk phases or from statistical analyses of the location of amino acids within globular proteins (Eisenberg, 1984). Current polarity scales for transbilayer helix prediction treat the bilayer as an isotropic nonpolar liquid 30 Å thick bounded by bulk water. The real situation is quite different from this; hydrated polar headgroup regions of the amphiphilic lipids separate the bulk water from the highly anisotropic hydrocarbon interior. While considerable attention has been paid to this issue in the context of the binding of small peptide hormones to bilayers by Schwyzer and his colleagues (Erne et al., 1985; Schwyzer, 1986; Sargent & Schwyzer, 1986), the complexities of the interfacial region are not generally taken into consideration when polarity plots are used for predicting membrane protein topology.

We have begun to examine these problems by studying the interactions of DMPC bilayers with hydrophobic tripeptides

†This work was supported by a grant from the National Science Foundation (DMB-8412754) and the American Heart Association—California Affiliate with funds contributed by the Orange County, CA, Chapter. R.E.J. is an Established Investigator of the American Heart Association. Parts of the research were carried out at Brookhaven National Laboratory, Upton, Long Island, NY, under the auspices of the U.S. Department of Energy with the additional support of the National Science Foundation.

*Author to whom correspondence should be addressed.

[1] Abbreviations: DMPC, 1,2-dimyristoyl-*sn*-glycero-3-phosphocholine; DOPC, 1,2-dioleoyl-*sn*-glycero-3-phosphocholine; K_p, partition coefficient in mole fraction units; PSRC, photosynthetic reaction center; IFH, interfacial hydrophobicity; *Rps.*, *Rhodopseudomonas*; *Rb.*, *Rhodobacter*.

0006-2960/89/0428-3421$01.50/0

of the form Ala-X-Ala-*O-tert*-butyl in which X = Gly, Ala, Leu, Phe, or Trp. We have measured the free energy of transfer of the Gly, Ala, Phe, and Trp peptides from water to DMPC vesicles and examined the phase behavior of tripeptide/lipid mixtures (Jacobs & White, 1986). The lipid partitioning and perturbing abilities of the peptides were found to increase with the surface area of the side chains. Interestingly, the free energies of transfer per unit residue area appeared to be about half the values of 20–25 cal/(mol·Å^2) expected for partitioning between water and bulk organic solvents (Reynolds et al., 1974; Richards, 1977). We subsequently examined in detail the effects of the peptides on the acyl chain motions of the DMPC and found that the perturbations increase as the size of the central (-X-) residue increases (Jacobs & White, 1987). However, we were unable to establish unambiguously whether the perturbations arose directly from peptide/hydrocarbon interactions or indirectly from peptide/headgroup interactions.

We report here the temperature dependence of the partitioning of the X = Leu, Phe, and Trp tripeptides from aqueous solution to DMPC bilayers, from which the enthalpies and entropies of transfer were determined. We also report neutron diffraction measurements which indicate in detail where the Trp tripeptide is located in oriented DOPC bilayers and how the bilayer is perturbed by the peptide. The thermodynamic constants are consistent with a hydrophobic interaction even though the diffraction results indicate that the most hydrophobic of the tripeptides is located in the headgroup region. A quantitative analysis of the binding suggests that 60–70% of the hydrophobic free energy has been consumed. This leads us to an extended analysis of the thermodynamics of helix insertion into bilayers with the interface as the "reference phase". The analysis suggests that adsorption of peptides at interfaces, even electrically neutral ones, is very favorable. We suggest that this adsorption may be important in helix formation and insertion. The analysis also emphasizes the crucial role of hydrogen bonding of side chains in the insertion process. Because one cannot be certain of the hydrogen bonding of a membrane protein of unknown three-dimensional structure, the precision of hydrophobicity scales is likely to be limited. We therefore introduce a "floating" interfacial hydrophobicity scale, IFH(h), which allows one to explore hydrogen bonding assumptions by varying the parameter h, which describes the extent of hydrogen bonding of polar side chains.

Materials and Methods

Binding Studies

Peptides were synthesized by standard methods as previously described (Jacobs & White, 1986). Radiolabeled amino acids and lipids were purchased from New England Nuclear (Boston, MA) and unlabeled lipids from Avanti Polar Lipids (Birmingham, AL).

Lipid vesicles used in all the partition coefficient (K_p) measurements were made by the method of Huang and Thompson (1974). Partition coefficients were measured by equilibrium dialysis using Spectrum Medical Industries (Los Angeles, CA) Teflon semimicro dialysis cells with a half-cell working volume of 1.0 mL and Spectra/Por 3 membranes with a nominal molecular weight cutoff of 3500. Lipid vesicles (^{14}C labeled) and peptide (^{3}H labeled) were allowed to equilibrate in the cells for 24 h. During this time the cells were rotated about an axis perpendicular to the membrane and immersed in a thermostated bath. Lipid and peptide concentrations in the two cell halves (one with lipid and one without) were determined via liquid scintillation counting and partition coefficients calculated as previously described (Jacobs & White, 1986).

Neutron Diffraction Studies

Instrumentation and Data Collection. The measurements were performed at Brookhaven National Laboratory on the H3A crystallography station (Schoenborn, 1983) at the High Flux Beam Reactor. The beam was collimated to 4-mm diameter and the diffractometer adjusted to have an approximately 1.4-m sample-to-detector distance (d_{sd}) so that d spacings could be determined with an accuracy and precision of ±0.3 Å corresponding to a single pixel on the two-dimensional detector. The precise d_{sd} was determined by using a National Bureau of Standards No. 675 d-spacing standard (synthetic fluorophlogopile mica, d_{001} = 9.98104 ± 0.00007 Å). Data were collected on a fixed-position 2D detector using conventional ω scans. The vertically mounted glass slide with the oriented sample was rotated through ω in 0.1° steps from 0 to 8° with respect to the beam. The detector and associated electronics record intensity (I_ω) versus 2θ for each value of ω. Four (h = 4) orders of lamellar diffraction data were easily observed from the oriented bilayers. Data were collected on the assumption that a fifth order would be observable under the same conditions, but this order was not seen. Evidence for the observability of orders six through eight was sought by setting ω to the Bragg condition for each of these peaks and increasing the counting time 10-fold. The diffraction peaks, if present, were still too weak to observe.

For each experimental sample, a complete set of ω scans was performed for 0, 10, and 20 mol % D_2O in the saturated salt solution used to maintain the relative humidity (RH).

Sample Preparation and Characteristics. All samples were prepared by using dioleoylphosphatidylcholine (DOPC) obtained from Avanti Polar Lipids (Birmingham, AL). Either A-W-A-*O-tert*-butyl or A-[*ring*-$^2H_5$] W-A-*O-tert*-butyl (1 per 10.0 lipids) was codissolved with the lipid in chloroform. The lipid/peptide mixtures were carefully deposited at the center of glass slides (6–7 mg of lipid) in a 1 cm by 4 cm rectangular pattern, and the chloroform was allowed to evaporate. The material was carefully respread to achieve a uniform distribution by using 2:1 $CHCl_3/CH_3OH$, which was allowed to evaporate in an air current free environment. Dry N_2 or Ar gas was then blown over the sample to remove remaining solvent. Samples were "annealed" at room temperature under Ar at 80–90% RH for approximately 48 h, which greatly reduced the mosaic spread. All data were collected at 66% RH (23 °C) from samples contained in a sealed aluminum chamber containing a saturated salt solution ($NaNO_2$). Whenever the chamber was opened to change samples or the salt solution, the system was allowed to come to equilibrium before data collection was begun. Equilibration was easily followed by short counts with ω set to the Bragg condition for h = 1–4. These intensities were measured before and after the data collection cycle to verify equilibration. The samples usually came to equilibrium in 1–2 h.

The DOPC/peptide mixtures formed highly ordered lattices as judged by $I_\omega(2\theta)$ diffraction peaks with a full width at half-maximum (fwhm) of 0.22°, which is essentially the same as the apparent fwhm of the undiffracted beam. This fwhm was observed for all diffraction orders. The mosaic spread due to angular distributions of the sample relative to the slide could be accurately represented by three Gaussian distributions with fwhm of about 0.3, 1.0, and 3.3° with relative amplitudes of 1.0:0.7:0.3. This distribution was remarkably reproducible from sample to sample.

Treatment of the Data. Observed structure factors $F_{obsd}(h)$

were obtained from the integrated intensities $I(h)$ by means of the equation:

$$[F_{obsd}(h)]^2 = I(h)\ A(h)\ G(h)\ L(h) \quad (1)$$

where $A(h)$, $G(h)$, and $L(h)$ are absorption, sample-beam intersection, and Lorentz corrections, respectively. $I(h)$ was determined by summing the background corrected $I_\omega(h)$ over the full range of ω. Because of the mosaic spread and because the scans were begun at $\omega = 0°$, I_ω for $\omega < 0°$ was lost for $h = 1$ and $h = 2$. The lost intensity, which accounted for 2% or less of the integrated intensity, was corrected for by fitting Gaussians to the observed intensities. $A(h)$ was obtained from measurements of the attenuation of the beam observed as the glass slide with and without sample was rotated through ω, by using standard equations (Peiser et al., 1960). $G(h)$ was obtained by straightforward geometrical calculations from the known geometry of the sample and the beam. Equation 1 is strictly correct only for mosaic spreads that are small compared to the range of ω. If this condition is not fulfilled, one should calculate the required correction at each ω by convoluting $A(h)\cdot G(h)$ with a mosaic spread function. We found, however, that for our case this correction procedure gave essentially the same result as the simpler one, and consequently we chose the simpler procedure.

The phases of the four diffraction peaks were confirmed to be −,−,+,− as expected from earlier measurements on DOPC bilayers (King et al., 1985; King & White, 1986) by plotting the $F_{obsd}(h)$ against the mole percent D_2O in the aqueous phase.

The structure factors $F_i(h)$ obtained for particular experimental conditions i (see Table II) were obtained from values calculated from the slopes and intercepts of linear least-squares fits of $F_{obsd}(h)$ versus mole percent D_2O. The errors reported for the $F_i(h)$ were taken as the larger of (1) the standard deviation of this least-squares fit or (2) the errors due to counting statistics propagated through all the corrections. The standard deviation of a background-corrected $I_\omega(h) = TC(h) - BC(h)$ was taken as $(TC + BC)^{1/2}$, where $TC(h)$ is the total counts within a region bounding $I_\omega(h)$ containing the diffracted intensity for order h and $BC(h)$ the background counts in a similar region not containing the diffracted intensity.

Data sets obtained from different samples were scaled to one another by using the difference structure factors $\Delta F_{wat}(h) = F_{Dwat}(h) - F_{Hwat}(h)$ for water as described by Büldt et al. (1979). One assumes $\Delta F_{wat}(h)$ is the same for all samples containing equal peptide concentrations and finds the scaling factor from an appropriate modification of eq 8 below.

Bilayer Profiles. The distribution $\rho_i(x)$ of matter across the width of the bilayer (x normal to the bilayer plane) in terms of neutron scattering length density for experimental condition i can be obtained from the equation (King et al., 1985):

$$\rho_i(x) = \rho_{0i} + \frac{1}{K_i}\frac{2}{d}\sum_h F_i(h)\cos(2\pi hx/d) \quad (2)$$

where K_i is a scale factor, d the Bragg spacing, and ρ_{0i} the average scattering length density of the unit cell and the sum extends over the number of measured diffraction orders (h = 1–4 in the present case). For the case of a bilayer containing two lipid molecules per unit cell which have an area S per molecule at the interface, the average scattering length density is given by

$$\rho_{0i} = \frac{2}{Sd}[n_w b_w(1-f) + n_w f b_d + n_p b_p + b_{lip}] \quad (3)$$

where n_w and n_p are, respectively, the numbers of waters and peptides per lipid, f is the fraction of deuterated water, and b_w, b_d, b_p, and b_{lip} are the scattering lengths for water, deuterated water, peptide, and lipid, respectively. The scattering lengths may be determined by summing the scattering lengths of the atoms in the molecule using the values published by Schoenborn (1975). The values used were (in units of 10^{-12} cm) $b_w = -0.18$, $b_d = +1.88$, $b_p = 7.88$ (13.03 if ring-$^2H_5$ deuterated), and $b_{lip} = 3.21$.

Equations 2 and 3 yield a scattering length density profile on an absolute scale providing S (or equivalently the mass density) is known. Because we are uncertain of S (King et al., 1985; White et al., 1987), we rewrite eq 2 in the form:

$$\rho_i(x)S = \rho_{0i}S + \frac{1}{k_i}\frac{2}{d}\sum_h F_i(h)\cos(2\pi hx/d) \quad (4)$$

where $k_i = K_i/S$. When k_i is properly chosen as described below, then $\rho_i(x)S$ gives the "scattering density" on what we refer to as the relative absolute scale. All profiles in this paper are reported with this scaling. The significance of this is that the true zero of the scattering length density is established as a reference level.

Scaling and the Determination of the Positions of Labeled Components. The basic experiment for determining the positions of labeled components is to determine the bilayer's structure factors $F_j(h)$ for the protonated (H) component and $F_i(h)$ for the deuterated component. The simplest, but least reliable, method of determining position is by means of eq 4, i.e., from $\rho_i(x)S - \rho_j(x)S$. Büldt et al. (1979) have noted that this method is subject to great uncertainties for low-resolution determinations (~12 Å) such as those reported here. The preferable method, and one that also yields the scale factor k_i, is to assume that the labeled component has a Gaussian distribution and to fit the difference structure factors $\Delta F_{ij}(h) = F_i(h) - F_j(h)$ to the structure factors obtained by Fourier transformation of the Gaussian distribution. This allows one to estimate group position and distribution to within an angstrom or better despite the low resolution (Büldt et al., 1979). This procedure is entirely analogous to the refinement methods used in crystallography (Woolfson, 1970).

We have found that neither the water (King & White, 1986) nor the peptide difference structure factors can be fit with a single Gaussian function. Both of these components appear to be best described by two Gaussians, one of which is located at the midplane ($x = d/2$) separating the headgroups (referred to as the bilayer "edge") and the other of which is located closer to the hydrocarbon core at $x = X_i$. In real space, over the interval $0 \le x \le d/2$, the scattering density distribution of either the water or the peptide is described by

$$\Delta\rho_{ij}(x)S = \frac{m_i b_i}{\sqrt{\pi}}\left[\frac{2g}{A_e}\exp\left[-\left(\frac{x-d/2}{A_e}\right)^2\right] + \frac{1-g}{A_i}\exp\left[-\left(\frac{x-X_i}{A_i}\right)^2\right]\right] \quad (5)$$

where we have adopted the convention $\Delta\rho_{ij}(x) = \rho_i(x) - \rho_j(x)$ to be consistent with our definition above of the difference structure factor $\Delta F_{ij}(h)$. Also, m_i is the number of deuterated components (peptide or water) per lipid, g is the fraction at the edge ($x = d/2$) position, A_e and A_i are the $1/e$ half-width of the Gaussians at the edge and at X_i, and b_i is the scattering length of the deuterated component. For the peptide, $m_i = n_p$ while for the water $m_i = fn_w$. The first term contains $2g$ rather than g because the water or peptide at the headgroup midplane assigned to one lipid molecule occupies only "half" of a Gaussian. The calculated difference structure factors

$\Delta F_{cij}(h)$ for the distribution are given by

$$\Delta F_{cij}(h) = 2m_i b_i[g \exp[-(\pi A_e h/d)^2](-1)^h + (1-g)\exp[-(\pi A_i h/d)^2]\cos(2\pi X_i h/d)] \quad (6)$$

The Gaussian parameters in eq 5 are varied to minimize the so-called residual (R) value given by

$$R = \frac{\sum_h ||k_{ij}|\Delta F_{cij}(h)| - |\Delta F_{ij}(h)||}{\sum_h |\Delta F_{ij}(h)|} \quad (7)$$

where k_{ij} is the scale factor given by

$$k_{ij} = \sum_h |\Delta F_{ij}(h)| / \sum_h |\Delta F_{cij}(h)| \quad (8)$$

Locating the Labeled Components Relative to Functional Groups of DOPC. To understand the effects of the peptide on the organization of the bilayer, it is desirable to locate the deuterated peptide and water relative to, say, the hydrocarbon core or the phosphate groups. King and White (1986) have reported neutron diffraction measurements on DOPC bilayers at 66% RH which permitted them to locate various functional groups of the DOPC. Their measurements provided eight (h = 8) diffraction orders with a resolution of ~6 Å. They subdivided the DOPC molecule into six functional domains consistent with this resolution, represented each domain by a Gaussian distribution, and fitted the calculated structure factors to the observed ones in the manner described in the previous section. Sufficient data were available from various specific deuteration experiments to permit them to construct the model with no arbitrary parameters. Provided that the perturbation of the bilayer by the peptide is not too large, this so-called quasi-molecular model for the DOPC permits one to estimate the effects of the peptide on the organization of the bilayer. Further, one obtains in the process scale factors that permit direct comparison of the real-space structures of the bilayers with and without peptide.

In the quasi-molecular model of DOPC, the molecule was divided into six parts as follows: Part 1 consisted of the terminal methyl groups, part 2 the seven $-CH_2-$ groups between the methyls and the double bonds, part 3 the double bonds, part 4 the next seven $-CH_2-$ groups, part 5 the ester linkages and the CH_2CH- of the glycerol moiety, and part 6 the remainder of the glycerol and the phosphorylcholine group. This model is shown in Figure 4 of King and White (1986). As a shorthand notation later in the paper, we will refer to parts 3, 5, and 6 simply as the C=C, C=O*Glyc, and PO_4*Chol groups, respectively.

King et al. (1985) and King and White (1986) reported the Bragg spacing of the DOPC bilayer at 66% RH as 49.7 ± 0.5 Å. However, that measurement was not made with the optimal spectrometer settings used in the present study. We therefore repeated the measurements of the d spacing using the same geometry as in the present study and found 49.1 ± 0.3 Å. With this more accurate measurement, we revised the quasi-molecular model parameters of King and White (1986) by scaling the A_j and X_j by the ratio 49.1/49.7, which had no effect on the R value of 0.024. King and White (1986) also assumed 6.0 waters/lipid on the basis of the measurements of Jendrasiak and Hasty (1974) on DOPC. However, subsequent radiotracer measurements of DOPC hydration in our lab as part of the study of White et al. (1987) gave a value of 5.36 ± 0.08, which is in complete agreement with the value of 5.4 determined by Elworthy (1961). We therefore used the value of 5.4 waters. Interestingly, by varying the n_w (g = constant in eq 5) in the quasi-molecular model, the R value passed through a minimum (R = 0.015) at precisely this value of n_w. This suggests that the amount of water in the bilayer structure can be estimated quite well from model building. The revised structural parameters for the DOPC bilayer at 66% RH are shown in Table III.

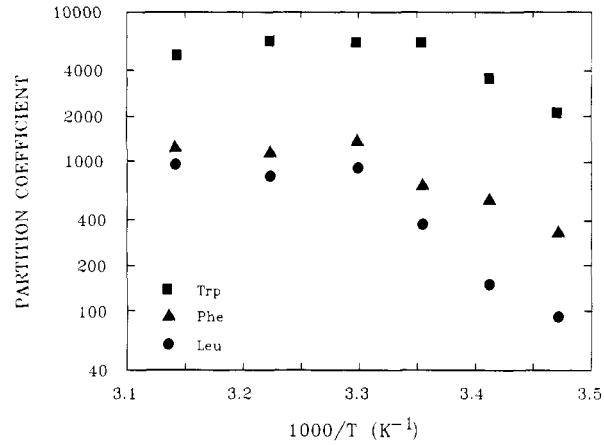

FIGURE 1: Plots of partition coefficient (K_p, mole fraction units) versus inverse temperature for peptides of the form A-X-A-*O-tert*-butyl with X = Trp, Phe, and Leu as noted. Thermodynamic constants noted in Table I for $T < T_M$ were derived from the slope and ordinate intercept of linear least-squares fits to the rightmost four points of each set.

We used the quasi-molecular model in the following way. We first scaled its A_j and X_j values to the Bragg spacing of 48.6 ± 0.3 Å we observed for the DOPC bilayer containing the tripeptide and represented it in real and reciprocal space by straightforward extensions of eq 5–8. We then extended the model to include the distributions of the water and peptide reported here. Assuming n_w = 5.4 as for the peptide-free bilayer, the R value increased to 0.11. Without making changes in the structural parameters of the water or peptide distributions, we then varied the values of n_w (keeping g in eq 5 fixed) and three, and only three, of the DOPC structural parameters for the peptide-containing bilayer. We found that an excellent fit (R = 0.012) could be obtained by changing slightly the width and location of the C=O*Glyc group and the width of the C=C distribution, and by reducing the amount of water as described under Results.

The error estimates reported for the distributions of water and peptide and for the locations of the quasi-molecular model functional groups were obtained as follows. For the peptide and water difference structures, the Guassian parameters were first optimized for the mean values of the difference structure factors. The structure factors were then allowed to range over their standard error ranges while reoptimizing the Guassian parameters to keep the R value fixed. The changes in the parameters were taken as the error ranges. When peptide and water distributions were added to the quasi-molecular DOPC model, the changes in the functional group distributions and n_w described above were made to minimize R. We then systematically varied each parameter to find the change necessary to double the value of R. These changes, which give one a feeling for the sharpness of the minimum in R or the sensitivity of the structure factors to the particular parameter, are reported as the likely uncertainties in the parameters.

RESULTS

Binding Studies. Figure 1 shows the temperature dependence of the partition coefficients (K_p) for peptides of the form Ala-X-Ala-*O-tert*-butyl with X = Trp, Phe, or Leu. High-temperature values are in agreement with previous measurements using the hygroscopic desorption method (Jacobs & White, 1986). Attempts to measure K_p for the X = Ala

Table I: Thermodynamic Constants for the Partitioning of the Tripeptides into DMPC Vesicles at 30 °C Derived from the Data of Figure 1 by Extrapolating to Temperatures above and below the Thermal Phase Transition Temperature (T_M) of DMPC[a]

	ΔG_t	ΔH_t	ΔS_t
$T > T_M$			
A-W-A-*O*-*t*-Bu	−5.12 ± 0.11	0	17.2
A-F-A-*O*-*t*-Bu	−4.24 ± 0.08	0	14.2
A-L-A-*O*-*t*-Bu	−4.10 ± 0.08	0	13.8
A-A-A-*O*-*t*-Bu[b]	−3.01 ± 0.03		
A-G-A-*O*-*t*-Bu[b]	−2.91 ± 0.03		
$T < T_M$			
A-W-A-*O*-*t*-Bu	−5.12 ± 0.11	18.7	79.8
A-F-A-*O*-*t*-Bu	−4.24 ± 0.08	15.5	68.2
A-L-A-*O*-*t*-Bu	−4.10 ± 0.08	27.4	108.6

[a] The units for ΔG_t and ΔH_t are kcal/mol and those for ΔS_t cal/(mol·K). *tert*-Butyl is abbreviated *t*-Bu. [b] Reference: Jacobs and White (1986).

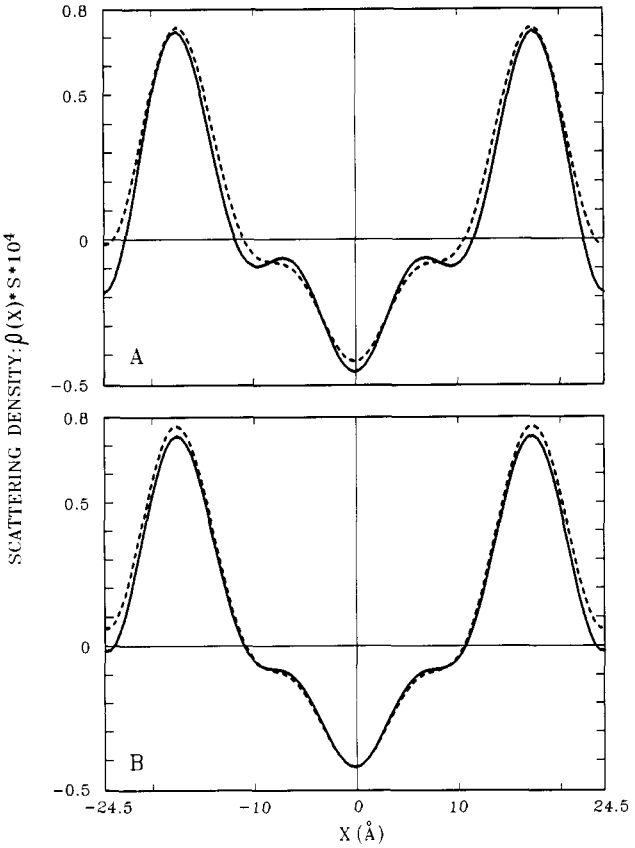

FIGURE 2: Neutron scattering density profiles of DOPC bilayers with and without A-W-A-*O*-*tert*-butyl. The profiles have been plotted on a relative absolute scale so that zero corresponds to the true zero of scattering length density (see Materials and Methods). (A) Profiles of bilayers with (dashed curve) and without (solid curve) peptide. Note that the presence of the peptide broadens the headgroup region asymmetrically and increases the scattering density in the water regions. The Bragg spacings of the DOPC and DOPC + peptide bilayers are 49.1 and 48.6 Å, respectively (66% RH, 23 °C). (B) Profiles of bilayers containing protonated (solid curve) or deuterated (dashed curve) A-W-A-*O*-*tert*-butyl. Notice the increased density in the headgroup region in the presence of the deuterated peptide. The peptide is deuterated with five deuteriums in the tryptophan.

peptide by the present method yielded small values (<100) with significant variation from experiment to experiment and will not be discussed further. The three data sets shown in Figure 1 have the same overall shape: horizontal at high temperatures with a break near the lipid phase transition temperature and a negative slope at lower temperatures. The lack of significant temperature dependence in the high-temperature regime indicates that the enthalpy of transfer (ΔH_t) of the peptides into the liquid-crystalline bilayer phase is approximately zero. Slopes and intercepts of the $K_p(1/T)$ curves yield the ΔH_t and ΔS_t values given in Table I. For all three peptides, the transfer to the liquid-crystalline bilayer is an entropy-driven process as expected for molecules partitioning as a result of the hydrophobic effect (Tanford, 1974).

Table II: Structure Factors $F_i(h)$ for the Four Observed Orders (h) of Diffraction Determined for Oriented Multilayers of DOPC Bilayers Alone and with A-[^{1}H]W-A-*O*-*t*-Bu (10.0:1) or A-[^{2}H]W-A-*O*-*t*-Bu (10.0:1) at 66% RH[a]

	$F_i(1)$	$F_i(2)$	$F_i(3)$	$F_i(4)$
no peptide				
i = 1[b], 0% D_2O	−68.0 ± 1.4	−38.3 ± 0.8	40.9 ± 0.8	−44.0 ± 0.9
i = 2, 20% D_2O	−99.5 ± 2.0	−14.7 ± 0.3	28.1 ± 0.6	−39.4 ± 0.8
with A-[^{1}H]W-A-*O*-*t*-Bu				
i = 3, 0% D_2O	−12.07 ± 0.04	−5.37 ± 0.02	5.78 ± 0.02	−5.43 ± 0.01
i = 4, 10% D_2O	−15.17 ± 0.04	−3.74 ± 0.02	5.10 ± 0.02	−5.19 ± 0.01
i = 5, 20% D_2O	−18.27 ± 0.04	−4.41 ± 0.02	5.28 ± 0.02	−4.95 ± 0.01
with A-[^{2}H]W-A-*O*-*t*-Bu				
i = 6, 0% D_2O	−13.39 ± 0.01	−5.14 ± 0.10	5.81 ± 0.02	−5.21 ± 0.01
i = 7, 10% D_2O	−16.56 ± 0.01	−3.55 ± 0.10	5.12 ± 0.02	−5.00 ± 0.01
i = 8, 20% D_2O	−19.74 ± 0.01	−1.96 ± 0.10	4.44 ± 0.02	−4.79 ± 0.01

[a] 0%, 10%, and 20% D_2O refer to the mole percent D_2O in the saturated $NaNO_2$ solution used to control the relative humidity of the multilayers. The Bragg spacing of the lamellar lattices is 49.1 ± 0.3 Å for DOPC bilayers alone and 48.6 ± 0.3 Å when peptide is present. [b] King and White (1986).

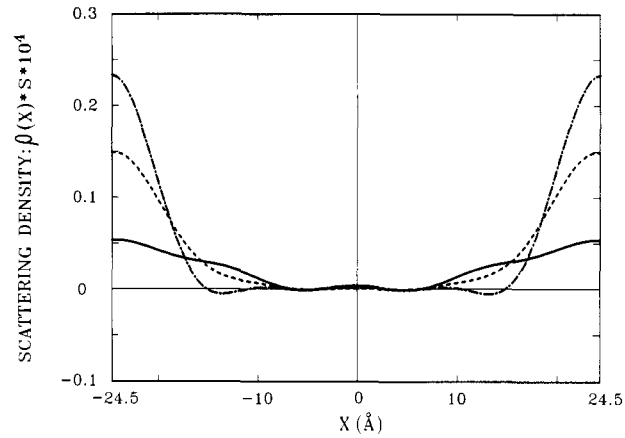

FIGURE 3: Scattering density profiles showing the distribution of the Trp-deuterated A-W-A-*O*-*tert*-butyl and deuterated water (10 mol % ^{2}H) in DOPC bilayers. These curves are constructed by Fourier transformation of the difference structure factors derived from the appropriate structure factors in Table II (see Materials and Methods). The solid curve (—) is the distribution of the 0.1 peptide/lipid, the dashed curve (---) the distribution of the 4.5 waters/lipid in bilayers containing the peptide, and the dot–dash curve (–·–) the distribution of the 5.4 waters/lipid in DOPC bilayers without peptide. Note that the water distribution shifts toward the hydrocarbon interior in the presence of peptide.

Neutron Diffraction. The structure factors for DOPC bilayers with and without protonated or deuterated A-W-A-*O*-*tert*-butyl and with varying percentages of D_2O are shown in Table II. The Bragg spacing of the bilayer decreases from 49.1 ± 0.3 to 48.6 ± 0.3 Å when the peptide is present. The structure factors and derivative difference structure factors of Table II were used to determine the scattering density profiles shown in Figures 2 and 3. In the remainder of the paper, for convenience, we will generally refer to the peptide

Table III: Structural Parameters Defining the Location of Various Components of DOPC Bilayers with and without A-W-A-*O-tert*-butyl[a]

component	b_i	DOPC alone, d = 49.1 Å		DOPC with peptide, d = 48.6 Å	
		X_i	A_i	X_i	A_i
2 CH_3	−0.96	0.0	3.06 ± 0.50	0.0	3.03 ± 0.50
14 CH_2	−1.40	5.43 ± 0.50	5.73 ± 0.70	5.38 ± 0.50	5.67 ± 0.70
2 C=C	1.12	8.40 ± 0.30	3.20 ± 0.70	8.31 ± 0.30	3.90 ± 0.30
14 CH_2	−1.40	10.87 ± 0.80	4.74 ± 0.50	10.76 ± 0.50	4.69 ± 0.30
C=O*Glyc	3.82	16.20 ± 0.20	2.77 ± 0.20	15.70 ± 0.10	2.90 ± 0.10
PO_4*Chol	2.03	20.15 ± 0.15	2.57 ± 0.40	19.95 ± 0.15	2.54 ± 0.40
water (total n_w = 5.4 ± 0.1)					
2.16	−0.39	20.93 ± 0.30	2.86 ± 0.10		
3.24	−0.58	24.55[b]	4.12[b] ± 0.10		
water (total n_w = 4.5 ± 0.2)					
3.5	−0.63			17.60 ± 0.80	6.70 ± 0.20
1.0	−0.18			24.30[b]	5.87[b] ± 0.05
peptide (n_p = 0.100)					
0.017 ± 0.003	0.13			12.80 ± 0.10	3.30 ± 0.80
0.083 ± 0.003	0.65			24.30[b]	8.80[b] ± 0.50

[a] The parameters describe Gaussian curves representing the distribution of the components across the thickness of the bilayer. A_i is the $1/e$ half-width in Å, X_i the location relative to the bilayer center in Å, and b_i the scattering length of the component in units of 10^{-12} cm. The parameters for the various submolecular parts of the DOPC bilayer alone are derived from King and White (1986) as described under Materials and Methods. The numbers associated with the components are numbers per lipid. [b] Values of $X_i = X_e$ and $A_i = A_e$, which are for "edge" locations corresponding to the midplane between opposing headgroups.

deuterated in the tryptophan ring as "deuterated peptide". However, the diffraction experiments do not provide explicit information on the disposition of the nondeuterated portions of the peptide.

Figure 2A compares the profiles of DOPC bilayers with and without the protonated peptide (dashed and solid curves, respectively). In both cases, there are two outer troughs corresponding to the water regions, two outer peaks corresponding approximately to the lipid glycerol backbone moieties in the opposing monolayers, and a central trough corresponding to the hydrocarbon core (Worcester & Franks, 1976; Büldt et al., 1979; King & White, 1986). The peptide has broadened the headgroup region asymmetrically toward the hydrocarbon region, somewhat "smeared" the hydrocarbon region, and elevated the scattering density in the water region. The changes are consistent with an increase in the area per lipid due to the presence of peptide in the water/headgroup region. This conclusion is supported by Figure 2B, which shows the profiles for bilayers containing protonated and deuterated peptide (solid and dashed curves, respectively). The important observation is that the increased scattering density of the sample containing the deuterated peptide (tryptophan) seems to be confined largely to the water/headgroup regions.

This can be seen more clearly from the peptide and water difference structures shown in Figure 3 (solid and dashed curves, respectively), which show clearly that water and peptide occupy the same region of the bilayer. Also shown in Figure 3 (dot–dash curve) is the difference water structure for the DOPC bilayer alone, which is known to contain about 5.4 waters per lipid (see Materials and Methods). The model building procedure described under Materials and Methods suggests that the presence of the peptide reduces the number of waters to about 4.5 per lipid, which is reflected in the difference in amplitude of the two curves. This number must be confirmed by direct measurements, but it is interesting to note that the volume of a peptide is about 600 $Å^3$, which is equivalent to about 20 water molecules. If the peptide simply displaced water from the interface, it would reduce the amount of water by 2 waters per lipid (there is 1 peptide per 10 lipids). The estimated number of waters lost is 1, suggesting that the peptide displaces about half of its volume in water. Another important conclusion that may be drawn from Figure 3 is that the peptide has broadened the water distribution toward the hydrocarbon region. This would be the logical result if some of the water associates with the peptide which spends some fraction of its time between the midplane of the headgroups and outer regions of the hydrocarbon core.

We note that the neutron diffraction data were obtained from oriented DOPC bilayers at low water contents while the partitioning data were obtained from DMPC bilayers in excess water. The peptide disposition could be somewat different at higher water contents and for bilayers formed as liposomes or vesicles rather than as oriented multilayers on glass surfaces. However, as we describe under Discussion, the two bilayer systems seem to respond similarly to the peptide and we believe the two systems to be quite similar.

Structure Refinement. The model building procedure outlined under Materials and Methods allows one to refine the diffraction analysis to arrive at a more quantitative description of the effect of the peptide on the bilayer. The results of the analysis are summarized in Table III and Figures 4 and 5. The approximate boundary of the hydrocarbon core is shown on the figures as an aid to interpretation. The location of this boundary is taken as the position of the C-2 carbons of the acyl chains which King and White (1986) found to be located approximately at X_5-A_5, where X_5 is the location of the C=O*Glyc group and A_5 is the $1/e$ half-width of the Gaussian distribution.

The peptide and water distributions in the bilayer can be described accurately by two Gaussian distributions, one distribution centered at the midplane of the headgroups of opposing bilayers (the "edge" distribution) and another (the "inner" distribution) closer to the hydrocarbon core. While not as extreme as when peptide is present, the water distribution in the peptide-free bilayer is also bimodal; a comparison of the location of the inner peak with the location of the PO_4*Chol group suggests that it is associated with the hydration of the PO_4 group. The water distributions are compared in Figure 4A. When peptide is present, both water distributions are broadened and the inner one makes a major shift toward the hydrocarbon core. Indeed, it appears that the water can now spend part of its time within the hydrocarbon region. This shift seems to be related to the distribution of the peptide, as can be seen in Figure 4B where the peptide and water distributions are compared.

Figure 5A shows the effect of the peptide on the DOPC molecule. As noted under Materials and Methods, we restricted changes in the DOPC structural parameters to the

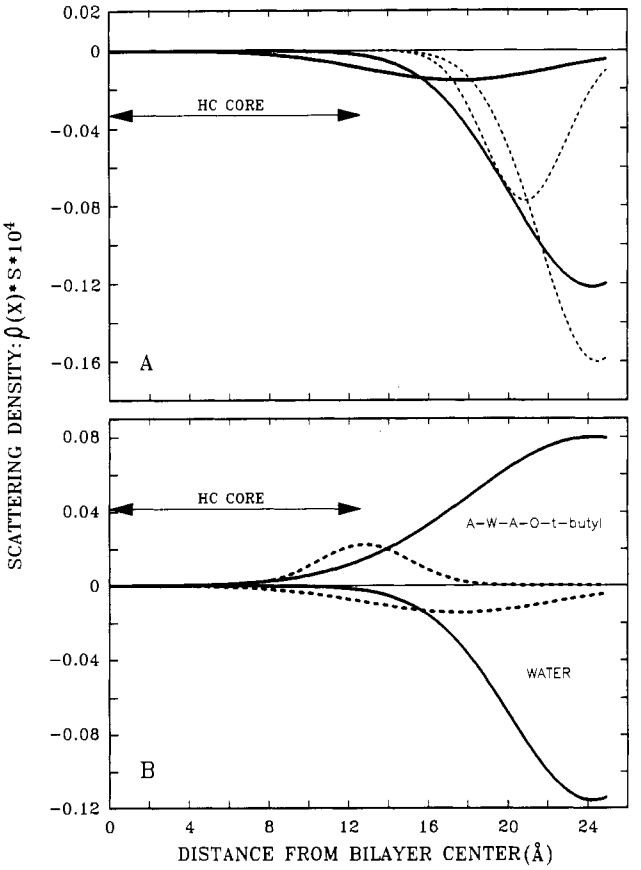

FIGURE 4: Gaussian curves representing the distributions of water and A-W-A-*O-tert*-butyl in DOPC bilayers. As described under Materials and Methods, the difference water and peptide structure factors can be accurately fitted in reciprocal space to two Gaussian distributions, one at the outer edge of the unit cell (midplane of opposing headgroups of adjacent bilayers) and another closer in to the hydrocarbon core. See Table III for the parameters of the Gaussian curves. The approximate extent of the hydrocarbon core is shown by the arrow (see text). (A) Comparisons of the water distributions with (solid curves) and without (dashed curves) peptide. Note that, in the presence of peptide, some of the water shifts into the hydrocarbon core region. (B) Comparisons of the distributions of peptide and water in DOPC bilayers. The upper curves (positive scattering density) are for the peptide and the lower curves (negative density) are for the water. The "edge" distributions are shown as solid curves and the "inner" distributions as dashed curves. Note that water distribution in the hydrocarbon region seems to mirror the peptide distribution, suggesting either that the water associated with the peptide directly or that the peptide has created defects in the hydrocarbon region which can be occupied by the water. The water appears to spend about 5% of its time in the hydrocarbon core while the Trp side chain spends about 13% of its time there (see text).

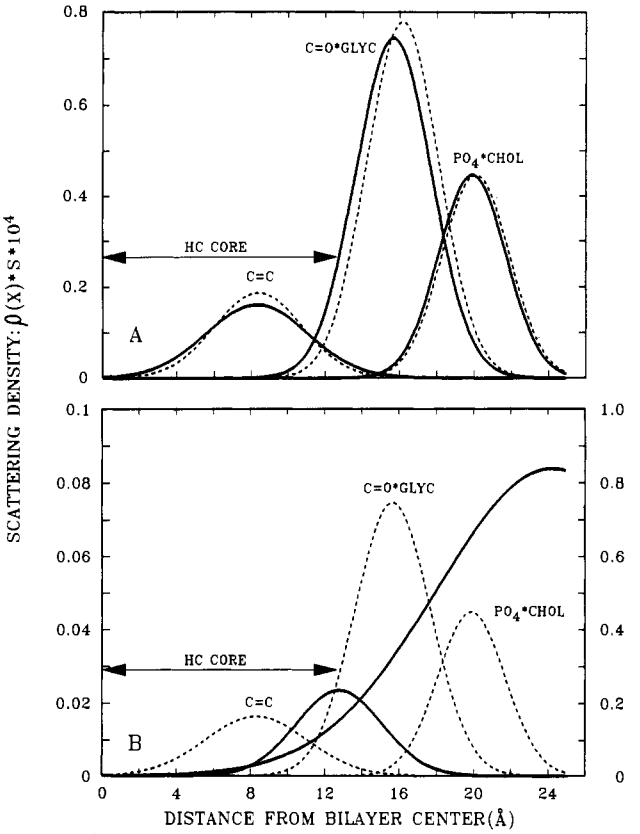

FIGURE 5: Changes in the distribution of the molecular groups of DOPC (A) and the relation of the molecular groups to the distribution of A-W-A-*O-tert*-butyl (B). See Materials and Methods for a description of the modeling procedure, based on the quasi-molecular model of King and White (1986), used to determine the distribution of the molecular groups. (A) Comparisons of the Gaussian representations of some of the molecular groups of the DOPC in the presence (solid curves) and absence (dashed curves) of peptide. The main effect of A-W-A-*O-tert*-butyl is to broaden slightly the double bond (C=C) distribution and to shift and broaden the carbonyl groups (C=O*Glyc) toward the bilayer center. These changes are consistent with an increase in the area/lipid of about 5%. The position and width of the phosphocholine group (PO_4*Chol) are only slightly affected while there is a significant shift in the positiono of the C=O*Glyc group. This suggests a slight headgroup reorientation. (B) Comparison of the distribution of A-W-A-*O-tert*-butyl (solid curves) with the distributions of some of the molecular groups (dashed curves). The scattering density scale for the molecular groups is 10-fold greater (right-hand scale) than that for the peptide (left-hand scale). Note that the inner distribution of the peptide is centered at the approximate headgroup/hydrocarbon boundary. The inner distribution accounts for 17% of the peptide and the outer distribution the other 83%.

double bond's Gaussian width and the width and location of the C=O*Glyc. The distributions of both groups broaden, and the C=O*Glyc shifts toward the bilayer center by about 0.5 Å. This shift is statistically significant because the structure factors of the model are more sensitive to the location of this group than any other (Table III). These changes in the C=C and C=O*Glyc are interpreted as a decrease in the hydrocarbon core thickness accompanied by an increase in the area per lipid of about 5%. Applying the method of Seelig and Seelig (1974) to our earlier deuterium NMR measurements (Jacobs & White, 1987), we estimate that A-W-A-*O-tert*-butyl causes a 6% increase in area when it interacts with DMPC liposomes (excess water; 5 lipids/peptide). This suggests that the behaviors of the oriented and unoriented systems are approximately equivalent.

The Bragg spacing of the bilayer changes by about 0.5 Å while the C=O*Glyc to C=O*Glyc spacing across the bilayer changes by about 1 Å. This is consistent with the fact that one need not shift the position of the PO_4*Chol group in the modeling procedure. This suggests that the PO_4*Chol to C=O*Glyc spacing increases in the presence of the peptide, possibly as a result of a small change in the average orientation of the headgroup.

The relationship of the peptide distribution to the headgroup and hydrocarbon core is shown in Figure 5B. Grossly, the deuterated peptide, specifically the tryptophan, is found between the double bond position and the edge of the bilayer. The two Gaussians suggest two average positions of the tryptophan, one located at the headgroup midplane accounting for 83% of the tryptophan and the other 11.5 Å from the midplane at the hydrocarbon/headgroup boundary accounting for the remaining 17%. One can estimate from the areas of the portions of the Gaussians which extend into the hydrocarbon core that 13% of the tryptophan is found in the hydrocarbon region. The distance from the center of mass of the tryptophan to the major axis of the fully extended peptide

can be estimated from CPK models to be 5.6 Å. If the major axis of the peptide were parallel to the bilayer plane and the peptide rotated 180° around this axis, the maximum separation of the tryptophan distibutions would be 11.2 Å, which is very close to the observed separation of the Gaussians. This would place the axis of the peptide roughly halfway between the C=O*Glyc and PO_4*Chol groups. A very large number of conformations of the peptide and headgroups undoubtedly exist, so this image is highly idealized.

Finally, returning to Figure 4B and comparing it to Figure 5B, one can see that the water is located well within the hydrocarbon core to about the depth of the double bonds. The portions of the Gaussian distributions of the water found in this region account for about 5% of the total. Examination of the water distribution of the peptide-free bilayer (Figure 4B) shows that the probability of finding water any deeper than about the center of the C=O*Glyc distribution is vanishingly small as expected from the low solubility of water in alkanes (Schatzberg, 1963). Schatzberg found the partition coefficient of water in alkanes to be about 5×10^{-4}, which is 2 orders of magnitude smaller than the apparent partition coefficient of the water between the headgroup and hydrocarbon region in the presence of peptide. We have considered the possibility that the scattering density we observe in the hydrocarbon core is due to the partial deuteration of the NH group of the Trp due to hydrogen–deuterium exchange. However, this effect can account for only about 3% of the scattering density.

Discussion

The peptide partition coefficient measurements reported here for $T > T_M$ are generally consistent with those of Jain et al. (1985), who have reported values of ΔG_t, ΔH_t, and ΔS_t for the binding of several short (2–6 AAs) Trp-containing peptides to DMPC bilayers. They showed the binding to be entropy driven and concluded from fluorescent spectroscopic measurements that the peptides were probably near the headgroup/hydrocarbon boundary, consistent with our diffraction results.

Below the gel to liquid crystalline transition ($T < T_M$), ΔH_t is significantly greater than zero and ΔS_t increases further (Table I). We have shown (Jacobs & White, 1987) that the peptides also cause significant disordering of the acyl chains of the DMPC below T_M which is consistent with the increases in both the enthalpies and entropies of transfer. We assume that the large enthalpy of binding results from the latent heat of acyl chain melting, which is favorably compensated for by the entropy increase resulting from the melting. Our results are different for $T < T_M$ than those reported by Jain et al. (1985) for the binding of their series of Trp-containing peptides with DMPC bilayers. They found virtually no change in ΔH_t or ΔS_t below the transition in apparent contradiction of the van't Hoff relationship for the distribution of the solute in the two coexisting phases at T_M. We have no explanation for the difference between our observations and theirs. Our present findings are consistent with our earlier calorimetric and NMR results (Jacobs & White, 1986, 1987).

The binding of the hydrophobic tripeptides to DMPC vesicles above the gel to liquid crystalline transition ($T > T_M$) is a clear example of the hydrophobic effect (Table I); the process has a large positive entropy of transfer with a negligible enthalpy (Tanford, 1974). The most hydrophobic tripeptide of the series (X = Trp) appears to be confined largely to the headgroup/water region of oriented DOPC bilayers with only occasional excursions of the tryptophan into the hydrocarbon core. We consider it quite likely that all the tripeptides we have examined spend little time in the hydrocarbon interior of the bilayer. There are several reasons for believing this. First, the free energy cost of inserting the charged amino group into the hydrocarbon core is likely to be 10–15 kcal/mol (Engelman & Steitz, 1981). Second, as discussed extensively below, the energetic cost of disrupting peptide hydrogen bonds with water is also prohibitive. There are three C=O and two NH groups which will require a total of about 15 kcal/mol (Roseman, 1988b) to insert into the hydrocarbon unless their hydrogen bonding capabilities can be satisfied internally. But the peptides are too short to have internally satisfied hydrogen bonds and therefore must remain out of the hydrocarbon interior. Third, the tryptophan is a large group which can visit both the outer region of the hydrocarbon core and the midplane of the headgroups relatively easily without having the peptide backbone enter the hydrocarbon region. With the exception of possibly phenylalanine, the other amino acids in the -X- position are less likely to be able to manage this. A counterargument might be that it is only the –NH group of the tryptophan which keeps it out of the hydrocarbon region. As we demonstrate below, however, the thermodynamic behavior of the series of tripeptides is quite linear as is their effect on acyl chain motions (Jacobs & White, 1987). Tryptophan does not deviate in its behavior compared to the other amino acid residues in the -X- position. We thus believe that the general structural features of the Trp-peptide/bilayer interaction will also be observed for the other tripeptides.

Our principal observation is that the peptides bind hydrophobically to phosphatidylcholine bilayer surfaces, and we conclude that a hydrophobic peptide need not enter the hydrocarbon core for the hydrophobic effect to be seen. In keeping with the general nature of the hydrophobic effect, the necessary condition is only that the hydrophobic group be removed from bulk water to alleviate the unfavorable entropy due to the local ordering of the surrounding water molecules. It is apparent that the headgroup/water region of the bilayer phase provides an environment for the hydrophobic groups that maximizes the entropy of the system. Our earlier calorimetric and NMR studies showed that the peptides tend to lower the phase transition temperature of DMPC and to cause a general disordering of the acyl chains of the bilayers (Jacobs & White, 1986, 1987). We can now see that these effects must be exerted largely through headgroup interactions which cause in part a slight increase in the area per lipid (about 5% for both oriented DOPC and liposomal DMPC) and consequently a disordering of the acyl chains.

One of the most surprising findings is the presence of a small but significant amount of water in the hydrocarbon core to the depth of the double bonds. There are 4.5 waters/lipid and 0.1 peptide/lipid. If 5% of the water is within the hydrocarbon core, then there are 2.3 waters/peptide associated with the hydrocarbon. We do not know how this occurs, but two possibilities are that the peptide (specifically the tryptophan) has water associated with it or that the local disordering of the hydrocarbon core creates defects which can be filled by water. If it is a general feature of peptide/bilayer interactions and if the effect is enhanced by larger peptides, the effect might be important for the insertion of helices into bilayers and for helix–helix interactions within bilayers because of the possible implications for hydrogen bonding.

Analysis of the Interfacial Binding of the Tripeptides. We have included in Table I our earlier measurements (Jacobs & White, 1986) of the water-to-DMPC ΔG_t's for A-X-A-*O*-*tert*-Bu with X = Gly and Ala in order to compare our results with those expected from several commonly used polarity

scales. The favorable free energies of transfer increase in the order Gly < Ala < Leu < Phe < Trp. This is consistent with our observation that K_p strictly increases as the surface area of the -X- residue increases (Jacobs & White, 1986) and is in complete accord with the Nozaki and Tanford (1971) scale. The sequence is not consistent with the GES scale (Engelman et al., 1986), which predicts Gly < Ala < Trp < Leu < Phe, or with the Kyte and Doolittle (1982) scale, which predicts Trp < Gly < Ala < Phe < Leu. It is significant that the location of Trp in the sequences has the greatest variability. Unlike the other members of the series, Trp has a substantial hydrophilic character. In general, one finds the largest differences among various polarity scales for those amino acids that have polar character but are uncharged. Even though Trp has the largest surface area and therefore the largest hydrophobic component of all the amino acid residues, the hydrophilic component can move it to a lower position on any polarity scale which assumes total immersion of the side chain in a nonpolar phase. In the present situation, however, Trp resides at an interface where its hydrophilic interactions are not disrupted even though the hydrophobic effect is clearly operating. We suggest that *interfacial* binding of Trp and the other amino acids of mixed hydrophobic/hydrophilic character is determined principally by the hydrophobic effect; the hydrophilic interactions remain largely satisfied at the interface and contribute only secondarily to the binding at electrically neutral interfaces.

Because the first step in the insertion of a peptide into a membrane must certainly involve the interface, it is useful to consider in detail the role of the interface in the insertion process. An important step in the analysis is the adoption of the interface as the reference "phase". Toward this end, we first compare the absolute values of the ΔG_t's we have measured for the transfer from bulk water to the interface (Table I) with those expected theoretically for the transfer from water to the interior of a thin hydrocarbon layer lacking a polar interface.

Prediction of the absolute values of ΔG_t is an uncertain business because several different contributions to ΔG_t must be considered as pointed out by Engelman and Steitz (1981) and Jähnig (1983). In general, five terms should be included in the water-to-oil ΔG_t:

$$\Delta G_t = \Delta G_{fob} + \Delta G_{fil} + \Delta G_{con} + \Delta G_{imm} + \Delta G_{lip} \quad (9)$$

These terms account for the hydrophobic effect (ΔG_{fob}), hydrogen bonding and other hydrophilic contributions (ΔG_{fil}), peptide conformational changes such as random coil to α-helix (ΔG_{con}), peptide immobilization effects (ΔG_{imm}), and lipid perturbation effects (ΔG_{lip}). These various contributions can be sorted out to some extent by considering how our measured values of ΔG_t, which we shall call ΔG_M, vary with ΔG_{fob} alone. That is, we initially make the naive assumption that polarization effects, H bonding, conformational changes, etc., are negligible. If a plot of ΔG_M against ΔG_{fob} yields a straight line, one can reasonably assume that incremental increases in ΔG_M are due to increases in the surface area (hydrophobicity) of the -X- residues. The intercept of the plot yields an estimate of the nonhydrophobic terms in eq 9.

Reynolds et al. (1974) refined a method of estimating ΔG_{fob} for the transfer of hydrocarbon molecules between water and a hydrocarbon phase based upon the surface area (A) of the molecules. They found that $\Delta G_{fob} = C_s A$, where C_s is a parameter with a value of −20 to −25 cal/(mol·Å^2) for saturated hydrocarbons. To adopt the general nomenclature of Eisenberg and McLachlan (1986), we will refer to C_s as the solvation parameter. This basic method has been useful for quantifying

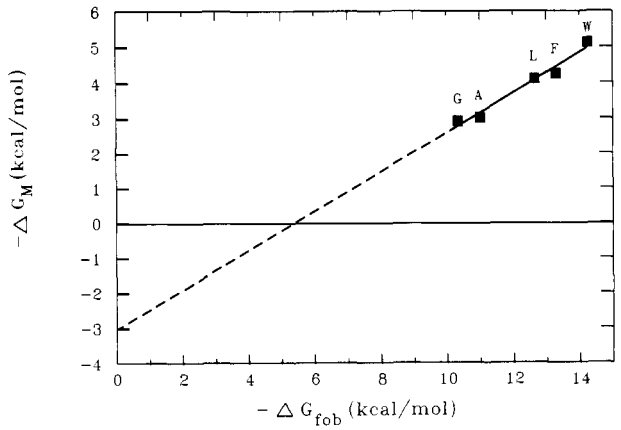

FIGURE 6: Comparison of the measured and theoretical free energies of transfer of amino acid residues from water to the bilayer. The measured free energy of transfer (ΔG_M) is from Table I, and the theoretical value is calculated from $\Delta G_{fob} = -22A_a$ (see text). The line is a least-squares linear regression with a slope of 0.56 ± 0.05 and an intercept of −3.0 ± 0.2 kcal/mol. One interpretation of these data is that 56% of the available hydrophobic free energy is used upon binding to the interface. The intercept free energy is the unfavorable free energy associated with adsorption.

the free energy of protein folding which results from burying hydrophobic amino acid side chains in the folding of proteins (Lee & Richards, 1971; Chothia, 1975; Rose et al., 1985) with C_s generally being taken as −22 cal/(mol·Å^2) (Richards, 1977).

We arrive at values of ΔG_{fob} by summing up the hydrophobic free energies of the individual residues based upon their accessible surface areas. Conveniently, it is common to calculate the accessible surface areas A_a of amino acid residues (-X-) of extended peptide chains by using Gly-X-Gly as a model (Shrake & Rupley, 1973; Chothia, 1976; Rose et al., 1985). We use the values of Rose et al. (1985) because they are based upon an ensemble average of the ϕ, ψ, and χ dihedral angles observed in proteins. This stochastic "standard state" is likely to be the better approximation for our unrestricted peptides in the bulk aqueous phase. We further assume that C_s = −22 cal/(mol·Å^2) and that the *tert*-butyl group has an accessible area twice that of a CH_3– (Reynolds et al., 1974; Harris et al., 1973). The value of ΔG_{fob} of A-X-A-*O*-*t*-Bu exclusive of the -X- is thus estimated to be −8.4 kcal/mol (water to bilayer); with -X- equal to Gly, Ala, Leu, Phe, and Trp, the respective ΔG_{fob}'s are −10.3, −11.0, −12.6, −13.3, and −14.3 kcal/mol.

Figure 6 shows $-\Delta G_M$ plotted against $-\Delta G_{fob}$; a clear linear relationship is apparent, consistent with the hydrophobic effect. The straight line (R^2 = 0.97) extrapolates to −3.0 ± 0.2 (SE) kcal/mol with a slope of 0.56 ± 0.05. The excellent linearity of the data in Figure 6 is consistent with the assumption that all thermodynamic interactions other than those involving -X- are equivalent among the five tripeptides. We interpret these numbers to mean that the hydrophobic effect is only 56% satisfied at the interface and that the terms ignored in eq 9 account for the +3.0 kcal/mol (water → bilayer) opposing the binding. Assuming that the hydrophilic interactions remain largely satisfied at the interface, the 3.0 kcal/mol must then be attributed to $\Delta G_{con} + \Delta G_{imm} + \Delta G_{lip}$.

The problem with the above analysis is that the slope of 0.56, which can be interpreted as the fraction (f) of the hydrophobic free energy consumed at the interface, depends upon the value of C_s assumed. For the hydrophobic free energy of transfer from water to the interface, which we shall call the interfacial hydrophobicity (ifh), we write

$$\Delta G_{ifh} = f\Delta G_{fob} = fC_s A_a \quad (10)$$

If $C_s = -12.4$, the value one would obtain by plotting ΔG_M against A_a, then $f = 1$ and the entire hydrophobic free energy in our experiment would be used by adsorption to the interface. Therefore, no further reduction in free energy would be obtained upon entry into the bilayer interior even if all the unfavorable hydrophilic terms were eliminated. This is unlikely and could be rectified by assigning a different C_s for the transfer from the interface to the bilayer interior. We find it simpler to adopt a single C_s and use the concept defined by eq 10. There are various estimates of C_s in the literature. In Richards' (1977) review he supposed the value would be very near to −20. Rose et al. (1985), from their values of A_a and the free energy of transfer measurements of Nozaki and Tanford (1971), arrived at values of 18.9 ± 0.7 and 20.1 ± 1.1 for the most hydrophobic amino acids depending upon whether they used the total accessible surface area or the amount of area buried. Importantly, in their plots of ΔG_t versus A_a, the more polar amino acids lie approximately on a parallel line which is shifted relative to the line through the nonpolar amino acids. Eisenberg and McLachlan (1986) have generalized this sort of approach to calculate so-called atomic solvation parameters for various polar and nonpolar surfaces of the side chains. Their value of C_s for the nonpolar amino acids is −16 ± 2. Given these results, the reasonable range of values for C_s is therefore −12.4 to −22.0, which leads to values of f of 1.0–0.56. The most likely range, −18 to −22, gives an f range of 0.7–0.6.

Interfacial Hydrophobicity Analysis of Peptide Insertion into Lipid Bilayers. It appears quite natural for peptides to associate with bilayer surfaces, which means that the surface must play an important role in the insertion of peptides into bilayers. We therefore examine the consequences of the interfacial hydrophobicity of amino acid residues and consider in detail the problem of transferring an amino acid residue of an extended peptide chain to the bilayer interior using the interface as the reference phase.

Consider the free energies of transfer from the interface to either the bulk aqueous phase or the bilayer interior. For the free energy of transfer from water to interface (ΔG_{wif}) we write

$$\Delta G_{wif} = \Delta G_{ifh} + \Delta G_a \qquad (11)$$

where ΔG_{ifh} is given by eq 10 and ΔG_a is the unfavorable water-to-interface free energy associated with the adsorption of the peptide to the bilayer which, from eq 9, can include contributions from ΔG_{con}, ΔG_{imm}, and ΔG_{lip}. ΔG_{fil} is taken as zero because we assume these interactions are not disrupted at the interface.

Similarly, for the free energy of transfer (ΔG_{ifi}) of an amino acid residue of an extended chain from the interface to the interior of the bilayer we write

$$\Delta G_{ifi} = [(1 - f)/f]\Delta G_{ifh} + \Delta G_{fil} + \Delta G_i \qquad (12)$$

The first term [$=(1 - f)\Delta G_{fob}$ from eq 10] represents the residual of the hydrophobic free energy which was not satisfied upon binding to the interface. The third term, ΔG_i, is the free energy of insertion arising from further changes in peptide and lipid conformations.

The general situation of amino acid residues at the interface as described by eq 11 and 12 is shown in Figure 7. The terms in eq 9, 11, and 12 that are concerned with conformational changes and immobilization effects of whole peptide chains cannot be easily dealt with at the present time but are discussed by Jähnig (1983). We consider in the remainder of the paper single amino acid residues and only the ΔG_{fob} and ΔG_{fil} terms, which can be taken as general indicators of the behavior of each residue. We consider the transfer of a residue of an

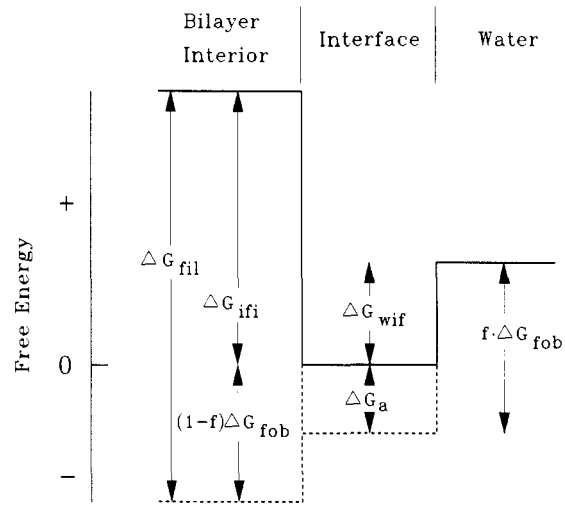

FIGURE 7: Free energy relationships for the binding of an amino acid residue at the bilayer surface. The reference "phase" is taken as the bilayer interface. For a residue at the interface, one must consider the probabilities of its going into the water phase or moving into the interior of the bilayer. ΔG_{wif} is the free energy of transfer from water to the interface composed of a fraction f of the hydrophobic free energy (ΔG_{fob}) available less the gain in free energy due to attachment at the interface (ΔG_a). ΔG_{ifi} is the free energy of transfer from the interface into the interior of the bilayer composed of the remainder $(1 - f)$ of the hydrophobic free energy and the unfavorable free energy due to the polar character of the amino acid residues (ΔG_{fil}) which includes the backbone NH and C=O groups. ΔG_{fil} determines the probability of the residue entering the bilayer because ΔG_{fob} is always favorable. ΔG_{fob} is the free energy of transfer of a residue from water to a completely nonpolar bulk solvent and is calculated from the surface area of the residue.

extended peptide chain from the water to the interior of the bilayer as part of an α-helix in three steps. The first step is the transfer of the peptide to the interface, which we assume to be described by eq 11 with $\Delta G_a = 0$. The second step is the transfer of the residue from the interface to the interior in the extended configuration so that the NH and C=O groups of the backbone are not hydrogen bonded. We assume this step to be described by eq 12 without the ΔG_i term. We will include in ΔG_{fil} the polar interactions of the side chains *and* the interactions of the NH and C=O groups on the backbone so that

$$\Delta G_{fil} = \Delta G_{bb} + \Delta G_{sc} \qquad (13)$$

where ΔG_{bb} and ΔG_{sc} represent the free energies associated with the transfer of the peptide backbone and side chain, respectively. In the third step, we introduce the favorable free energy change (ΔG_{hfr}) associated with the formation of hydrogen bonds involving both backbone ($-\Delta G_{bH}$) and side-chain ($-\Delta G_{sH}$) polar groups. We describe this last step by the equation:

$$\Delta G_{hfr} = -\Delta G_{bH} - \Delta G_{sH} \qquad (14)$$

We will be interested in comparing the free energy of transfer ($\Delta G_{ext} = \Delta G_{ifi} - \Delta G_i$) of a peptide from the interface to bilayer interior as an extended chain with the comparable free energy of transfer ($\Delta G_{hlx} = \Delta G_{ext} + \Delta G_{hfr}$) as a helix.

To investigate the thermodynamics of transfer using eq 11–14, we must evaluate ΔG_{fob}, ΔG_{fil}, ΔG_{bH}, and ΔG_{sH}. This is not a trivial problem, as discussed in detail by Roseman (1988a). The major problems concern group additivity, so-called "self-solvation" and "proximity" effects, and, ultimately, the choice of organic solvents for the determination of transfer free energies relevant to the bilayer interior. These problems cannot be easily solved at the present time; ultimately, one

needs direct information on the solubility of a large number of model peptides in bilayers. Despite the possible problems discussed by Roseman (1988a), we use simple group additivity assumptions to calculate the free energies until appropriate direct measurements are available. We estimate ΔG_{fil} using the general approach of Engelman and Steitz (1981); we adopt their protocol for calculating the free energy of transfer of charged groups and some of their values for the transfer of polar groups (OH, 4.0 kcal/mol; $-NH_2$, 5.0 kcal/mol; COOH, 4.3 kcal/mol; C=O, 2.0 kcal/mol). For the polar contributions due to the backbone NH and C=O, we use the recent results of Roseman (1988b) which indicate that the free energy of transfer from water to a nonpolar solvent of a bonded —NH···O=C— pair is 0.55 kcal/mol and that of an unbonded pair is 6.12 kcal/mol. For an unbonded pair, we attribute 2.0 kcal/mol to the C=O and therefore 4.12 kcal/mol to the NH. If the conclusions of Roseman (1988a) are correct, these numbers are likely to be upper limits.

We take into account the free energies associated with hydrogen bond formation in the following way. The formation of a helix is assumed to result in the pairing of all the hydrogen bonds on the backbone except for Pro which will leave an unbonded C=O group so that $-\Delta G_{bH} = -6.12 + 0.55 = -5.57$. Accounting for the hydrogen bonding of the polar portions of side chains is more problematic. We shall assume that, on average, a fraction h of the hydrogen bond forming side-chain polar groups are involved in hydrogen bonds and examine the consequences of different choices of h. Taking $h = 0$ will mean that no side chains are involved in hydrogen bonds while $h = 1$ will mean that all of the hydrogen bond forming groups of the side chains form hydrogen bonds. We somewhat arbitrarily designate hydrogen bond forming groups for each side chain in a manner that reasonably rank orders the polarity of the side chains as follows. We assume that all of the polar groups of the side chains (including Pro because of its unbonded NH group) can make hydrogen bonds unless the group is charged, which excludes Lys, Asp, and Glu but includes Arg because of its additional NH and NH_2 groups. Further, if the side chain has two hydrogen bonding groups (Asn, Gln, His, Arg), we assume that only one hydrogen bond will be formed. To introduce these assumptions into our equations, we define $-\Delta G_{sH} = -h\Delta G'_{sc}$, where $\Delta G'_{sc} = 0$ if the side chain has a single polar moiety that is charged, (0.5) $(\Delta G_{sc} - \Delta G^*_{sc})$ if the side chain has two uncharged polar groups, and $(1.0)\Delta G_{sc}$ if the side chain has a single uncharged polar group. In these definitions, ΔG^*_{sc} is the free energy of transfer of the charged group of the side chain should it have one as does Arg.

The final set of equations, describing respectively the free energy of transfer from water to interface, from interface to interior as an extended chain, and from interface to interior as a helix, are

$$\Delta G_{wif} = fC_sA_a \quad (15)$$

$$\Delta G_{ext} = (1 - f)C_sA_a + \Delta G_{bb} + \Delta G_{sc} \quad (16)$$

$$\Delta G_{hlx} = \Delta G_{ext} - \Delta G_{bH} - h\Delta G'_{sc} \quad (17)$$

The values of ΔG_{bb}, ΔG_{sc}, ΔG_{bH}, and $\Delta G'_{sc}$ for each residue used in the calculations are summarized in Table IV. Finally, we must select for use in the equations a value of C_s from which f is determined by $-12.4/C_s$ [recalling that the slope of the curve in Figure 6 is (0.563)(22) = 12.4]. Rather than selecting a preferred value of C_s, however, we examined the consequences of various choices.

We calculated ΔG_{wif}, ΔG_{ext}, and ΔG_{hlx} for each residue for $h = 0$ or 1 assuming $C_s = -12.4$, -16, -19, or -22 (corresponding, $f = 1.0$, 0.77, 0.65, or 0.56). The results are shown for each residue in Figure 8. The amino acids have been rank-ordered along the abscissa in the order of increasing A_a on the basis of the values of Rose et al. (1985). The data points corresponding to side chains with polar groups are black, and those corresponding to side chains without polar groups are shaded dark gray. The data "points" are shown in Figure 8B,C as rectangles whose vertical dimensions represent the spreads of the free energy resulting from the different values of C_s.

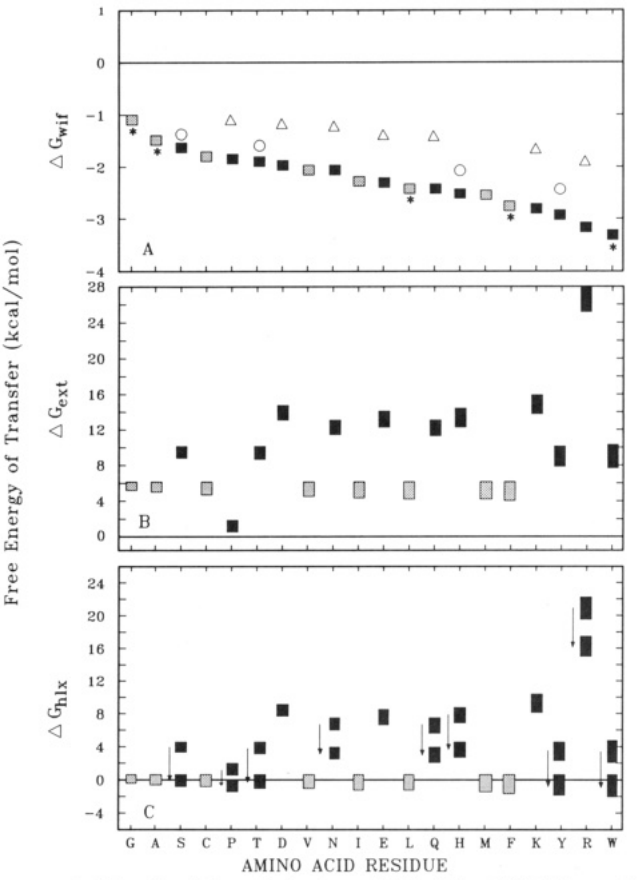

FIGURE 8: Results of the calculations of (A) ΔG_{wif}, (B) ΔG_{ext}, and (C) ΔG_{hlx} using eq 15, 16, and 17, respectively, and the data of Table IV. The black data points identify polar side chains and the dark gray points the nonpolar side chains. (A) The points marked with an asterisk (*) are those determined experimentally in this paper. The black and dark gray points were calculated by assuming $C_s = -12.4$ cal/(mol·Å^2) and $f = 1$ (see text). The two sets of points indicated by open circles and open triangles are hypothetical values based upon the measurements of Rose et al. (1985) to explore the assumption that C_s may be different for the moderately and very polar residues (see text). Note that ΔG_{wif} is always negative, suggesting that all amino acid residues will tend to bind at bilayer interfaces even in the absence of charged lipids. (B) ΔG_{ext} assumes the polar groups of the side chains and backbone are not hydrogen bonded. The data "points" are shown as rectangles whose lengths indicate the results of allowing C_s to range from -12.4 to -22 cal/(mol·Å^2); the uppermost end is the value for $C_s = -12.4$. Note that the free energy is always positive regardless of the C_s value as long as no hydrogen bonds are made. It is very unlikely that a peptide chain can enter a bilayer without having the hydrogen bonds satisfied (Engelman & Steitz, 1981). (C) ΔG_{hlx} is derived from ΔG_{ext} by accounting for hydrogen bonding of peptide backbone in an α-helical configuration and permitting varying degrees of hydrogen bonding of polar side chains as determined by the parameter h; $h = 0$ means no hydrogen bonding, and $h = 1$ means full hydrogen bonding of permitted groups (see text). Note that all of the nonpolar residues have negative values of free energy as long as $C_s \leq -16$ cal/(mol·Å^2); otherwise, the general result is not strongly dependent on C_s. Certain of the polar side chains will have favorable free energies of transfer depending upon the extent of hydrogen bond formation. The change in ΔG_{hlx} with hydrogen bonding from $h = 0$ to $h = 1$ is indicated by the arrows.

Table IV: Summary of the Various Free Energies of Transfer (Water to Oil) Used in Equations 15–17 To Calculate the ΔG_{wif}, ΔG_{ext}, and ΔG_{hlx} Shown in Figure 8 and the IFH(h) Interfacial Hydrophobicity Scales of Table V[a]

amino acid	A_a	ΔG_{sc}	ΔG_{bb}	ΔG_{fil}	ΔG_{bH}	$\Delta G'_{sc}$
Gly	88.1	0.00	6.12	6.12	5.57	0.00
Ala	118.1	0.00	6.12	6.12	5.57	0.00
Ser	129.8	4.00	6.12	10.12	5.57	4.00
Cys	146.1	0.00	6.12	6.12	5.57	0.00
Pro	146.8	0.00	2.00	2.00	0.00	2.00
Thr	152.5	4.00	6.12	10.12	5.57	4.00
Asp	158.7	8.60	6.12	14.72	5.57	0.00
Val	164.5	0.00	6.12	6.12	5.57	0.00
Asn	165.5	7.00	6.12	13.12	5.57	3.50
Ile	181.0	0.00	6.12	6.12	5.57	0.00
Glu	186.2	8.00	6.12	14.12	5.57	0.00
Leu	193.1	0.00	6.12	6.12	5.57	0.00
Gln	193.2	7.00	6.12	13.12	5.57	3.50
His	202.5	8.24	6.12	14.12	5.57	4.12
Met	203.4	0.00	6.12	6.12	5.57	0.00
Phe	222.8	0.00	6.12	6.12	5.57	0.00
Lys	225.8	9.80	6.12	15.92	5.57	0.00
Tyr	236.8	4.00	6.12	10.12	5.57	4.00
Arg	256.0	21.62	6.12	27.74	5.57	4.50
Trp	266.3	4.12	6.12	10.24	5.57	4.12

[a] ΔG_{sc} is the free energy of transfer for the polar groups of the side chains and ΔG_{bb} the free energies for the backbone polar groups. ΔG_{bH} is the favorable free energy change occurring when NH···O=C bonds are made between backbone groups as a result of helix formation and $\Delta G'_{sc}$ the maximum favorable free energy change that can occur as a result of polar side chain hydrogen bond formation (see text). Proline is a special case because of its missing NH on the backbone; we assume $\Delta G_{bH} = 0$ and treat the C=O group as a polar side chain. The stochastic accessible surface areas (A_a) in Å^2 are used for calculating the hydrophobic free energy (ΔG_{fob}) and are taken from the work of Rose et al. (1985). The group free energies are based upon the work of Engelman and Steitz (1981) and Roseman (1988b). Consult text for specific details.

The effect of varying h from 0 to 1 is shown in Figure 8C by using two rectangles related by an arrow with the rectangle near the tail representing $h = 0$ and the rectangle near the head representing $h = 1$.

The free energies of transfer from water to interface are shown in Figure 8A. In this case the free energies of transfer are calculated only with $C_s = -12.4$ because this is the experimentally determined solvation parameter for binding to the interface [$fC_s = (-12.4/C_s)C_s$]. The amino acids whose free energies of transfer are reported in this paper are marked with an asterisk. All values of ΔG_{wif} are negative in this plot, which emphasizes that there will be a general tendency for all residues to bind at the interface. A possibly important observation is that the four residues with the largest ΔG_{wif}, Lys, Tyr, Arg, and Trp, are also very polar. These residues therefore have amphipathic characteristics. Their high hydrophobicities will tend to drive them onto the interface, but their high polarities will tend to keep them out of the hydrocarbon interior. This means they will have a special propensity for the bilayer interface, and we speculate below that peptide segments rich in these residues may act as interface "stays" during helix insertion. Interestingly, Cornette et al. (1987) have noted that Arg, Trp, and Tyr (but not Lys) tend to be on the hydrophobic faces of amphipathic helices, which may be due in part to their amphipathic character.

We do not know that the interfacial C_s of −12.4 will be correct for all of the residues because we examined, with the exception of Trp, only the side chains without polar groups. It is possible that C_s will change somewhat with the polarity of the side groups, and we therefore include this possibility in Figure 8A. Shown as open circles and open triangles are estimates of possible ΔG_{wif} values based upon the work of Rose et al. (1985) who measured the average fraction of accessible surface area each of the 20 amino acids bury upon folding in 23 proteins. The fraction buried depended upon the type of residue, and they found that the residues fell into three groups: nonpolar (Gly, Ala, Cys, Val, Ile, Leu, Met, Phe, and Trp), moderately polar (Ser, Thr, His, and Tyr), and very polar (Pro, Asp, Asn, Glu, Gln, Arg, and Lys). Graphs of the accessible surface area against the average area buried showed that the groups fell on straight lines with slopes of 1.0, 1.2, and 1.7. Plotting the data in this way is equivalent to the treatment of our data shown in Figure 6 except our plot is, essentially, of area buried versus accessible area, i.e., the reciprocal of Rose et al.'s plots. Their findings suggest a relationship between our results and the thermodynamics of burying residues in folded proteins. We take the behavior of the residues observed by Rose et al. as a possible indicator of the differences we might expect in future experiments concerned with more polar side chains. In Figure 8A, C_s has been divided by 1.2 for Rose et al.'s moderately polar residues (open circles) and by 1.7 for the very polar residues (open triangles). To the extent that our experiments and Rose et al.'s are equivalent, it is clear that different values of C_s will not alter our general conclusions and will have only a moderate effect quantitatively.

A final caution is that we do not yet know the extent to which C_s will depend upon lipid headgroup. If the phosphatidylcholine group (specifically the choline) has a much more hydrophobic character than other phospholipid headgroups, as suggested by Dill and Stigter (1988), C_s could be smaller for phosphatidylethanolamine, for example. However, this view of the phosphatidylcholine headgroup is not in accord with the Homan and Pownall's (1988) measurements of the transbilayer diffusion ("flip-flop") of pyrene-labeled phosphatidylcholines. They found that the flip-flop rates and associated activation energies increased in the order phosphatidylcholine (PC) < phosphatidylglycerol (PG) < phosphatidic acid (PA) < phosphotidylethanolamine (PE). On the other hand, Homan and Pownall found that the HPLC retention times of the phospholipids on a stationary nonpolar phase increased in the order PA < PG ≪ PE < PC. The likely behavior of a particular headgroup as a "solvent" for peptides is thus unclear and can be resolved only by direct measurements.

Figure 8B shows the results of the calculations of ΔG_{ext}. All of the values are positive including the nonpolar side chains because of the unsatisfied hydrogen bonds. This plot emphasizes the crucial importance of satisfying hydrogen bonds if a peptide is to enter the bilayer (Engelman & Steitz, 1981). Further, this result is clearly independent of the choice of the value of C_s chosen and supports strongly our earlier conclusion that all of the tripeptides in our series are likely to be outside the hydrocarbon core even if one ignores the charge on the amino terminus.

The nonpolar amino acid residues will be able to enter the bilayer interior only if they can adopt a configuration that satisfies their hydrogen bonds as shown in Figure 8C. The obvious and likely configuration that will satisfy this requirement is the α-helix (Engelman & Steitz, 1981). The most striking feature of Figure 8C is the behavior of Pro, Trp, Ser, Thr, and Tyr. As can be seen, the hydrogen bond status of the polar groups of these residues totally determines their behavior. In terms of membrane protein structure, it is clear that the opportunity for these groups to form hydrogen bonds within a helix or a group of helices will have a large effect on the thermodynamics of insertion. We note that we have assumed that those groups capable of forming two hydrogen

bonds form at most one; relaxing this assumption to permit more hydrogen bonding would allow His, Asn, and Gln to behave more like nonpolar groups. Examining again the effect of the choice of C_s, one can see that the choice is not a critical one as long as $C_s \leq -16$. The final question concerns the values we used in the calculations of ΔG_{fil}. We do not know the precise values that should be used for bilayers as opposed to bulk nonpolar solvents. However, one can see from Figure 8C that the general conclusions will be the same even if the values are in error by several kcal/mol. We can conclude that Gly, Ala, Cys, Val, Ile, Leu, Met, and Phe will always favor helix insertion; Ser, Pro, Thr, Tyr, and Trp may or may not depending on hydrogen bonding patterns; Asp, Asn, Glu, Gln, His, Lys, and Arg will generally not favor insertion. Most hydrophobicity scales are, of course, largely consistent with this conclusion. As we noted earlier, though, the greatest variation among the scales arises with the moderately polar residues. It is clear that their placement on a scale will be critically affected by the hydrogen bonding assumptions.

Implications for Protein Insertion into Bilayers. Many questions remain unanswered about the sequence of events between translation on the ribosome and the assumption of the final folded state of the protein in the bilayer. There seems to be considerable variation in the timing of translation and insertion; in some cases insertion seems to begin before translation is complete while in other it occurs posttranslationally [see reviews by Wickner and Lodish (1985), Rothman and Kornberg (1986), Schatz (1986), Coleman and Robinson (1986), and Wickner (1988)]. Among the many important questions is that of the metabolic requirements for insertion. Frequently, a transmembrane potential must exist, and often ATP is consumed during insertion or transport. However, assuming that membrane proteins exist in situ in their lowest free energy state as do globular proteins, one must suppose that the main functions of the electrochemical potential and ATP consumption are to accelerate insertion. The spontaneous insertion of proteins into bilayers is entirely reasonable on thermodynamic grounds as discussed thoroughly by a number of workers (von Heijne & Blomberg, 1979; Engelman & Steitz, 1981; Weinstein et al., 1982; Jähnig, 1983; Briggs & Gierasch, 1986). None of our results are inconsistent with spontaneous insertion as long as hydrogen bonding needs can be satisfied. We therefore assume spontaneous insertion in the following discussion.

A major question is that of the extent to which the protein folds before insertion. Given the results presented here, one must consider seriously the possible role of peptide/interface interactions in the insertion process. We suggest in Figure 9 a general pattern for the insertion of multihelix proteins into membranes beginning with a largely unfolded chain as one might encounter during or shortly after exit from the ribosome. Certain portions of the peptide are likely to associate particularly strongly with the bilayer interface due to the combination of a large negative ΔG_{wif} and a large positive ΔG_{hlx}. The preference of these regions (stays) of the peptide chain for the interface may increase the chances of amide and carbonyl groups finding one another to initiate α-helix formation. Helix formation would presumably be aided by the reduction in the accessible surface areas of the residues, which can provide a free energy decrease of about 2 kcal/mol per residue (Chothia, 1976). This scheme suggests that the bilayer interface may act as a catalytic surface for helix formation with the energy being provided by the hydrophobic effect. The very nonpolar helices can make further energetic gains by moving to the bilayer interior due to the remainder of the hydrophobic free

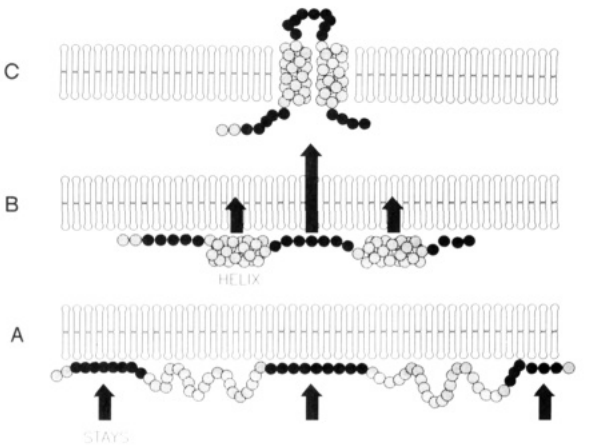

FIGURE 9: Hypothetical scheme for the formation and insertion of transmembrane helices via helix formation at the bilayer interface. (A) The peptide chain will have a general tendency to bind to the bilayer interface. This binding may reduce the degrees of freedom of the chain sufficiently to enhance the formation of intrapeptide hydrogen bonds leading to helix formation. Certain regions of the peptide chain rich in charged and other polar groups with large hydrophobicities will have a strong tendency to associate with the surface and act as "stays" (interface anchors) (see text). (B) The reduction of the degrees of freedom of the peptide at the interface may increase the chances of intramolecular hydrogen bonds necessary for helix formation. The formation of the helix is highly favored because of the reduction in the exposed surface area of residues that accompanies helix formation (Chothia, 1976). (C) The membrane "stays" of lowest polarity can cross the membrane in conjunction with the very nonpolar regions of the helices as helical hairpins (Engelman & Steitz, 1981).

energy $[(1 - f)C_sA_a]$ and by possible gains from the disordering of the bilayer. The membrane stays, distributed at intervals along the chain, have the smallest chance of crossing the membrane and thus act as pivots around which the helices rotate as they pass through the bilayer. Those stays that do cross as parts of "helical hairpins" (Engelman & Steitz, 1981) must be the less polar ones and could be aided by a transmembrane potential (Weinstein et al., 1982). Another issue to consider is that of asymmetries in transmembrane lipid distribution, which are now widely recognized as a general feature of membrane organization [see reviews by Bretcher (1973), Rothman and Lenard (1977), and Bergelson and Barsukov (1977)]. These asymmetries and specific lipid/peptide interactions may have an effect on insertion.

In this scheme, the residues with large values of ΔG_{wif}, which are simultaneously very polar and hydrophobic, play a special role. Uppermost in the scale are tryptophan, arginine, lysine, and tyrosine. The basic amino acids are clearly important. This is in complete accord with the charge-cluster hypothesis of Weinstein et al. (1982) concerning the voltage-dependent insertion of peptides into bilayers and the "comparative anatomy" of N-terminal topogenic protein sequences (von Heijne, 1986a). The combined effects of their hydrophobicity and possibly strong interactions with negative membrane surface charge will make the basic amino acids potent membrane stays.

Certain peptides that do not form α-helices in solution have a greater tendency to do so in the presence of the bilayer interface on the basis of observations made on the tridecapeptide dynorphin$_{1-13}$ (Erne et al., 1985; Schwyzer, 1986) and on the tetracosapeptide ACTH$_{1-24}$ (Gremlich et al., 1983, 1984; Gysin & Schwyzer, 1984; Sargent & Schwyzer, 1986). Both of these peptides have random coil configurations in solution but apparently adopt α-helical conformations in certain regions upon binding to neutral phosphatidylcholine bilayers. The situation with ACTH$_{1-24}$ is particularly inter-

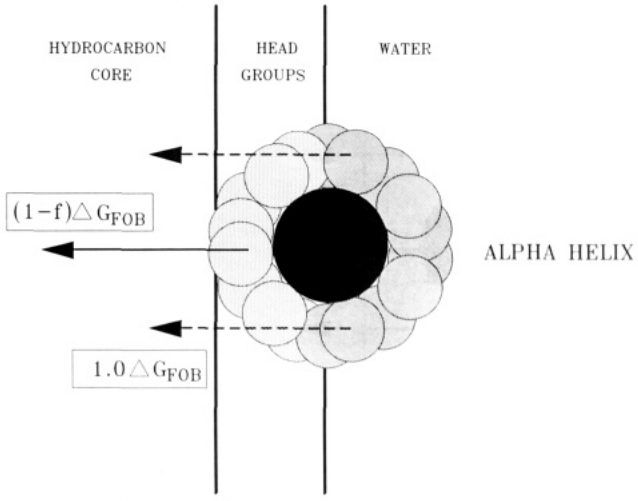

FIGURE 10: Schematic drawing of an α-helix (end view) associated with the bilayer interface indicating the strong free energy gradient driving a nonpolar helix into the bilayer interior. Even if the helix is not formed at the surface (Figure 9) but arrives as a preformed unit, there should still be a strong tendency to bind to the bilayer surface as a first step toward insertion. The geometry of the interface is such that an α-helix with bulky nonpolar side chains can be half-buried at the interface between the polar headgroup and the hydrocarbon core (see text, Figure 5B, and Table III).

esting. Schwyzer and his colleagues have shown that the helix forms in $ACTH_{1-10}$ and partially inserts into the bilayer while $ACTH_{11-24}$ is in an extended configuration on the bilayer surface. They have also shown that the 11–24 segment is essential for binding the peptide to the bilayer even though it is highly charged and the bilayer is neutral. The amino acid sequence of this segment is -Lys-Pro-Val-Gly-Lys-Lys-Arg-Arg-Pro-Val-Lys-Val-Tyr-Pro-, which satisfies the requirements of a membrane stay segment.

While we do not know with certainty the role the interface might play in membrane protein folding, the interface is likely to be important even if portions of the peptide are already folded into an α-helix before or during the approach to the bilayer. The arguments for the role of the interface are the same regardless of the peptide chain's secondary structure. Thus, the notion (Briggs et al., 1986) of leader sequences formining β structures at a bilayer or monolayer surface is equally plausible. We consider in Figure 10 the interaction of a helix with a bilayer interface. Interestingly, the distance from the PO_4*Chol group to the hydrocarbon core of DOPC is about 8 Å (Figure 5A), which is roughly half the diameter of a helix comprised of residues with bulky hydrophobic side chains (a polyglycine α-helix is about 7 Å in diameter; a fully extended Ile side chain is 5–6 Å). Thus, a helix can be about half buried at the interface with half of its residues in the interface and half out as shown in Figure 10; there will be a strong free energy gradient driving the helix into the bilayer. This view of helix insertion immediately suggests a mechanism for the insertion of synthetic amphipathic helices which apparently form voltage-dependent ion channels (Lear et al., 1988; Ohki et al., 1988). One can easily visualize in Figure 10 polar groups on the side of the helix facing the water poised to be driven into the bilayer by an electric field interacting with the helix dipole and/or charges on the hydrophilic surfaces.

Interfacial Hydrophobicity (IFH) Polarity Scales. The thermodynamic analysis of the insertion of helices resulted in values of ΔG_{hlx} for each amino acid residue. These values can be considered as a hydrophobicity scale and, like the many other hydrophobicity scales, may be useful for locating the likely transmembrane helix-forming regions of membrane proteins of unknown three-dimensional structure. While we are hesitant to propose yet another polarity scale for this purpose, the explicit consideration of the polar side chain hydrogen bonds gives one the ability to introduce this important consideration into transmembrane helix searches. Michel et al. (1986) considered the relative abundance of the amino acids between the helices and connecting links of PSRCs and commented that the problem of general helix-predictive schemes is that they do not take into account the different functions of a protein such as chloride transport in halorhodopsin, proton transport in bacteriorhodopsin, sodium ion transport in sodium channels, etc. In particular, they noted that while Tyr is underrepresented in the helices of the PSRC, it is probably overrepresented in bacteriorhodopsin for possibly functional reasons. The neutron diffraction studies of Engelman and Zaccai (1980) and Rogan and Zaccai (1981) suggest that bacteriorhodopsin has a hydrophilic interior. These ideas suggest that internal hydrogen bonding in bacteriorhodopsin may be particularly important and that the hydrophobicity scale appropriate for bacteriorhodopsin may not be entirely appropriate for the PSRC. There is thus some merit in having a "floating" polarity scale that allows one to explore systematically the consequences of side-chain hydrogen bonding patterns.

To be consistent with common practice, we define the interfacial hydrophobicity index such that positive index values correspond to the nonpolar amino acids. Therefore, we write

$$\text{IFH}(h) \text{ index} = -\Delta G_{hlx}(h) \qquad (18)$$

Before the scales can be explicitly derived, one must consider what value of C_s to use in the calculations. The values arrived at by Rose et al. (1985) and Eisenberg and McLachlan (1986) were derived from partition coefficients obtained from reasonably polar organic phases (alcohols). The interior of the bilayer is much more likely to be equivalent to an alkane bulk phase. Therefore, we suggest that the C_s values of −20 to −25 cal/(mol·Å^2) obtained by Reynolds et al. (1974) are likely to be most appropriate. As Richards (1977) did, we choose a value of −22 as a reasonable median value.

We show in Table V the IFH(h) indexes for $h = 0$, 0.5, and 1. We include in the table the so-called distribution coefficients (ϕ) of Michel et al. (1986) which describe the relative abundance of each residue in helices compared to connecting links of PSRCs. Chothia (1976) found in his survey of the general properties of globular proteins that the fraction of the polar groups engaged in hydrogen bonds was 0.5 independent of molecular weight. Therefore, we take the $h = 0.5$ scale as the most likely median scale, and we have rank ordered the amino acids according to decreasing values of IFH(0.5). Comparing the IFH(0.5) values with the ϕ values shows that only four amino acids, Pro, His, Thr, and Ser, are "misplaced" in the sense that only these have IFH(0.5) < 0 and $\phi > 1$. However, we note that perfect agreement in this sense could be obtained by making very specific hydrogen bonding assumptions.

A Transmembrane Helix Search Example. Each of the transmembrane helices of the PSRCs of *Rps. viridis* and *Rb. sphaeroides* has a hydrophobic domain of at least 19 amino acids (Deisenhofer et al., 1985; Allen et al., 1987) which are apparently within the hydrocarbon core the bilayer (Yeates et al., 1987). It is of interest to examine the polarity plots of these helices by using the IFH(0.5) index. As an example, we show in Figure 11 a hydropathy plot of the L subunit of *Rb. sphaeroides* constructed with a 19-AA sliding-window average using the microcomputer spread-sheet method of

Table V: Interfacial Hydrophobicity [IFH(h)] Scales for h = 0, 0.5, and 1 and Relative Distribution Coefficients of Amino Acids between Transbilayer Helices and Their Connecting Links for Photosynthetic Reaction Centers[a]

amino acid	IFH(0)	IFH(1)	IFH(0.5)	ϕ[b]
phenylalanine (F)	1.60	1.60	1.60	1.21
methionine (M)	1.41	1.41	1.41	2.51
leucine (L)	1.31	1.31	1.31	1.77
isoleucine (I)	1.19	1.19	1.19	1.83
valine (V)	1.04	1.04	1.04	1.24
cysteine (C)	0.86	0.86	0.86	16.55
alanine (A)	0.59	0.59	0.59	1.94
proline (P)	−0.59	1.41	0.41	**0.25**
glycine (G)	0.30	0.30	0.30	**0.93**
tryptophan (W)	−2.10	2.02	−0.04	**0.81**
tyrosine (Y)	−2.27	1.73	−0.27	**0.27**
threonine (T)	−3.08	0.92	−1.08	1.09
serine (S)	−3.30	0.70	−1.30	1.60
glutamine (Q)	−5.69	−2.19	−3.94	**0.38**
asparagine (N)	−5.95	−2.45	−4.20	**0.38**
histidine (H)	−6.84	−2.72	−4.78	1.49
glutamate (E*)	−6.76	−6.76	−6.76	**0.30**
aspartate (D*)	−7.62	−7.62	−7.62	**0.02**
lysine (K*)	−8.17	−8.17	−8.17	**0.28**
arginine (R*)	−19.70	−15.14	−17.42	**0.74**

[a] The IFH(h) index is defined as $-\Delta G_{blx}(h)$ (eq 17 and 18), where h refers to the average fraction of polar side group hydrogen bonds made. The solvation constant C_s is taken as −22 cal/(mol·Å^2). See text for details. The scales are rank ordered for the IFH(0.5) scale. Residues with polar character are shown in boldface, and those with charge at pH = 7 have an asterisk (*). The units of the IFH scales are kcal/mol. The distribution coefficients (ϕ) describe the relative frequency of the amino acids in the transbilayer helices of three PSRCs relative to connecting links determined by Michel et al. (1986). Values of ϕ < 1.0 are shown in boldface type. [b] Reference: Michel et al. (1986).

Vickery (1987). The plot clearly reveals five peaks associated with the five known transmembrane helices (indicated by solid horizontal bars lettered A–E). Those regions most likely to form helices are those with an average IFH(0.5) index greater than zero. It should be noted that a single point on such a plot represents the average index of 19 amino acids. Therefore, the minimum criterion for a potential helix-forming region is that a single point be found above the zero axis. Further, because the region of the helix with the highest average IFH(0.5) index is the region that is most likely to be membrane spanning, one would suppose that the maximum IFH(0.5) point in each putative helical domain is most likely to represent the helix center. Shown in Figure 11 are the 19-residue domains selected by this criterion (light lines with marked centers below the known helix locations). Maxima occurred at AA numbers 40, 92, 125, 186, and 241; the 19 amino acids corresponding to these maxima are 31–49, 83–101, 116–134, 177–195, and 232–250. None of these regions include any of the very polar amino acids (His, Gln, Asn, Glu, Asp, Lys, and Arg) and correspond well to the known helices (A, 32–55; B, 83–111; C, 116–138; D, 171–198; E, 225–250) found by Allen et al. (1987). No polarity plot by itself can be expected to select the precise ends of the helices which can be very polar (e.g., helix B). The IFH(0.5) index plot as implemented here satisfies the minimum qualification of a successful hydropathy plot, namely, that the most likely transbilayer domains be selected.

It is interesting to consider the IFH(0.5) plot in Figure 11 in the context of the problem of protein insertion into bilayers. Examination of the minima in the curve reveals that they are not of equal depth. Minima 1 and 5 are the deepest, minima 2 and 4 are the shallowest, and minimum 3 is intermediate. In addition, the N-terminus (minimum 1) has a lower index than the C-terminus (minimum 6). These relationships, which are also observed in the H and L subunits (data not shown),

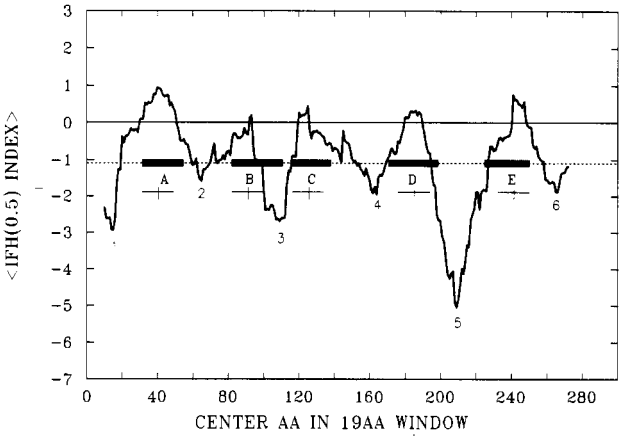

FIGURE 11: Hydropathy plot of the L subunit of the photosynthetic reaction center of *Rb. sphaeroides* using the IFH(0.5) (Table V) hydrophobicity scale with a 19 amino acid sliding-window average. The known helix locations (Allen et al., 1987) are shown as heavy horizontal lines marked below with the helix designation (A–E). The dashed line indicates the average IFH(0.5) index for the whole subunit. The criterion for a region of the chain to be a potential transmembrane helix is that a single point (representing the average hydrophobicity of 19 residues) be located above the zero line. The point in a positive region with the maximum ⟨IFH(0.5)⟩ represents the most hydrophobic 19 residue sequence and is thus most likely to be the region of the peptide spanning the hydrocarbon core of the bilayer. The light lines below the heavy ones are the regions selected in this manner; the vertical crossline indicates the location of the local ⟨IFH(0.5)⟩ maximum.

are more apparent in narrow window (5–11 AAs; data not shown). The peptide passes back and forth across the bilayer in a fashion that places the N- and C-termini on opposite sides of the membrane. The passages across are such that minima 1, 3, and 5 are on the N-terminal (cytoplasmic) side of the photosynthetic membrane and minima 2, 4, and 6 are on the C-terminal (periplasmic) side. Michel et al. (1986) have already noted that helix termini and connecting links on the periplasmic side contain considerably fewer acidic and basic residues than those on the cytoplasmic side. This distribution appears to be a general feature of bacterial inner membrane proteins (von Heijne, 1986b). The polarity plots clearly reveal this situation. The relative probabilities of the various regions of the peptide entering the membrane may be reasonably accurately predicted by the plots so that the relative IFH(0.5) averages of the regions may indicate the insertion protocol: the nonpolar helices would tend to cross first followed by the less polar stays while the most polar stays would cross only with great difficulty. This suggests the helical hairpin insertion in a pairwise manner with the AB helices and CD helices constituting insertion pairs; presumably, E would have to cross with the relatively less polar C-terminus (compared to N-terminus) perhaps aided by the transmembrane potential. We note that the end termini of both the L and M subunits of the reaction centers are negatively charged.

A final matter to be considered in helix insertion is that the overall hydrogen bonding pattern of the peptide may change during the insertion process. It is not unreasonable to hypothesize that the hydrogen bonding patterns of the peptides could differ before, during, and after insertion in a manner that favors the final folded form of the peptide which is reasonably the lowest energy configuration of the membrane protein.

SUMMARY

We have demonstrated that tripeptides of the form Ala-X-Ala-*O-tert*-butyl bind at the surface of bilayers with ther-

modynamic parameters characteristic of simple hydrophobic interactions. There is a linear relationship between the free energy of binding and the surface area of the -X- amino acid residue. Our measurements for -X- = Gly, Ala, Leu, Phe, and Trp lead us to conclude that the peptides find a favorable environment at the interface which reduces their hydrophobic free energy about 60% compared to the free-solution values. At the same time, it appears likely that hydrophilic interactions remain largely satisfied. There are clear similarities between interfacial binding of amino acid residues and the burying of residues in folded globular proteins. Binding at the interface can be viewed as an intermediate step in the insertion process. After binding, the amino acid residues have available a favorable free energy change for insertion equivalent to about 40% of the free-solution hydrophobic free energy. Opposing this favorable free energy are the hydrophilic interactions which must be, finally, interrupted upon insertion. We take the view that the bilayer interface is a reasonable reference "phase" for the insertion process. This leads to a detailed consideration of the thermodynamics of insertion which identifies the importance of hydrogen bonding. This analysis leads to "floating" interfacial hydrophobicity scales IFH(h) which allow one to construct hydropathy plots based upon different assumptions about the hydrogen bonding patterns of the polar side chains. We also suggest a special role for residues such as Arg, Lys, Trp, and Tyr which are simultaneously very polar and very hydrophobic; these will have the highest probability of being found at the interface. Regions of peptide chains rich in such groups may act as "stays" which stabilize nascent peptide chains at the interface and act as nucleation sites for protein folding and insertion. Even in the absence of a special nucleation role for the interface, the same general principles of adsorption we observe for the tripeptides should apply to α-helices. There is likely to be a strong free energy gradient for a helix partially embedded at the bilayer interface which will act to drive the helix deeper into the bilayer.

ACKNOWLEDGMENTS

We are pleased to acknowledge the excellent technical assistance of April Diaz and many stimulating discussions with Dr. Glen King in the early phases of the diffraction work. We thank Dr. Michael Wiener for his comments on the manuscript.

Registry No. DMPC, 18194-24-6; DOPC, 4235-95-4; Ala-Gly-Ala-*O*-*tert*-butyl, 100859-29-8; Ala-Ala-Ala-*O*-*tert*-butyl, 65356-57-2; Ala-Leu-Ala-*O*-*tert*-butyl, 92752-43-7; Ala-Phe-Ala-*O*-*tert*-butyl, 100859-30-1; Ala-Trp-Ala-*O*-*tert*-butyl, 100859-31-2.

REFERENCES

Allen, J. P., Feher, G., Yeates, T. O., Komiya, H., & Rees, D. C. (1987) *Proc. Natl. Acad. Sci. U.S.A. 84*, 6162–6166.
Bergelson, L. D., & Barsukov, L. I. (1977) *Science 197*, 224–230.
Bretcher, M. S. (1971) *J. Mol. Biol. 59*, 351–357.
Bretcher, M. S. (1973) *Science 181*, 622–629.
Briggs, M. S., & Gierasch, L. M. (1986) *Adv. Protein Chem. 38*, 109–180.
Briggs, M. S., Cornell, D. G., Dluhy, R. A., & Gierasch, L. M. (1986) *Science 233*, 206–208.
Büldt, G., Gally, H. U., Seelig, J., & Zaccai, G. (1979) *J. Mol. Biol. 134*, 673–691.
Chothia, C. (1975) *Nature (London) 254*, 304–308.
Chothia, C. (1976) *J. Mol. Biol. 105*, 1–14.
Coleman, A., & Robinson, C. (1986) *Cell 46*, 321–322.
Cornette, J. L., Cease, K. B., Margalit, H., Spouge, J. L., Berzofsky, J. A., & DeLisi, C. (1987) *J. Mol. Biol. 195*, 659–685.
Deisenhofer, J., Epp, O., Miki, K., Huber, R., & Michel, H. (1985) *Nature (London) 318*, 618–624.
Dill, K. A., & Stigter, D. (1988) *Biochemistry 27*, 3446–3453.
Eilers, M., & Schatz, G. (1986) *Nature (London) 322*, 228–232.
Eisenberg, D. (1984) *Annu. Rev. Biochem. 53*, 595–623.
Eisenberg, D., & McLachlan, A. D. (1986) *Nature (London) 319*, 199–203.
Elworthy, P. H. (1961) *J. Chem. Soc. (London)*, 5385–5389.
Engelman, D. M., & Zaccai, G. (1980) *Proc. Natl. Acad. Sci. U.S.A. 77*, 5894–5898.
Engelman, D. M., & Steitz, T. A. (1981) *Cell 23*, 411–422.
Engelman, D. M., & Steitz, T. A. (1982) in *The Protein Folding Problem* (Wetlaufer, D. B., Ed.) pp 87–113, Westview Press, Boulder, CO.
Engelman, D. M., Steitz, T. A., & Goldman, A. (1982) *Methods Enzymol. 88*, 81–88.
Engelman, D. M., Steitz, T. A., & Goldman, A. (1986) *Annu. Rev. Biophys. Biophys. Chem. 15*, 321–353.
Erne, D., Sargent, D. F., & Schwyzer, R. (1985) *Biochemistry 24*, 4261–4263.
Gremlich, H.-U., Frigeli, U.-P., & Schwyzer, R. (1983) *Biochemistry 22*, 4257–4264.
Gremlich, H.-U., Frigeli, U.-P., & Schwyzer, R. (1984) *Biochemistry 23*, 1808–1810.
Gysin, B., & Schwyzer, R. (1984) *Biochemistry 23*, 1811–1818.
Harris, M. J., Higuchi, T., & Rytting, J. H. (1973) *J. Phys. Chem. 77*, 2694–2703.
Henderson, R., & Unwin, P. N. T. (1975) *Nature (London) 257*, 28–32.
Homan, R., & Pownall, H. J. (1988) *Biochim. Biophys. Acta 938*, 155–166.
Huang, C.-H., & Thompson, T. E. (1974) *Methods Enzymol. 32*, 485–501.
Jacobs, R. E., & White, S. H. (1986) *Biochemistry 25*, 2605–2612.
Jacobs, R. E., & White, S. H. (1987) *Biochemistry 26*, 6127–6134.
Jähnig, F. (1983) *Proc. Natl. Acad. Sci. U.S.A. 80*, 3691–3695.
Jain, M. K., Rogers, J., Simpson, L., & Gierasch, L. M. (1985) *Biochim. Biophys. Acta 816*, 153–162.
Jendrasiak, G. L., & Hasty, J. H. (1974) *Biochim. Biophys. Acta 337*, 79–91.
King, G. I., & White, S. H. (1986) *Biophys. J. 49*, 1047–1054.
King, G. I., White, S. H., & Jacobs, R. E. (1985) *Biochemistry 24*, 4637–4645.
Kuntz, I. D. (1972) *J. Am. Chem. Soc. 94*, 4009–4012.
Kyte, J., & Doolittle, R. F. (1982) *J. Mol. Biol. 157*, 105–132.
Lear, J. D., Wasserman, Z. R., & DeGrado, W. F. (1988) *Science 240*, 1177–1181.
Lee, B., & Richards, F. M. (1971) *J. Mol. Biol. 55*, 379–400.
Lenard, J., & Singer, S. J. (1966) *Proc. Natl. Acad. Sci. U.S.A. 56*, 1828–1835.
Michel, H., Weyer, K. A., Gruenberg, H., Dunger, I., Osterhelt, D., & Lottspeich, F. (1986) *EMBO J. 5*, 1149–1158.
Nozaki, Y., & Tanford, C. (1971) *J. Biol. Chem. 246*, 2211–2217.
Ohki, S., Danho, W., & Montal, M. (1988) *Proc. Natl. Acad. Sci. U.S.A. 85*, 2393–2397.

Peiser, H. S., Rooksby, H. P., & Wilson, A. J. C. (1960) *X-ray Diffraction by Polycrystalline Materials*, Chapman & Hall, London.
Reynolds, J. A., Gilbert, D. B., & Tanford, C. (1974) *Proc. Natl. Acad. Sci. U.S.A. 71*, 2925–2927.
Richards, F. M. (1977) *Annu. Rev. Biophys. Bioeng. 6*, 151–176.
Rogan, P. K., & Zaccai, G. (1981) *J. Mol. Biol. 145*, 281–284.
Rose, G. D. (1978) *Nature (London) 272*, 586–590.
Rose, G. D., & Roy, S. (1980) *Proc. Natl. Acad. Sci. U.S.A. 77*, 4643–4647.
Rose, G. D., Geselowitz, A. R., Lesser, G. J., Lee, R. H., & Zehfus, M. H. (1985) *Science (Washington) 229*, 834–838.
Roseman, M. A. (1988a) *J. Mol. Biol. 201*, 513–522.
Roseman, M. A. (1988b) *J. Mol. Biol.* 201, 621–623.
Rothman, J. E., & Lenard, J. (1977) *Science 195*, 743–753.
Rothman, J. E., & Kornberg, R. D. (1986) *Nature (London) 322*, 209–210.
Sargent, D. F., & Schwyzer, R. (1986) *Proc. Natl. Acad. Sci. U.S.A. 83*, 5774–5778.
Schatz, G. (1986) *Nature (London) 321*, 108–109.
Schatzberg, P. (1963) *J. Phys. Chem. 67*, 776–779.
Schoenborn, B. P. (1975) *Brookhaven Symp. Biol. 27*, I10–I17.
Schoenborn, B. P. (1983) *Acta. Crystallogr. A39*, 315–321.
Schwyzer, R. (1986) *Biochemistry 25*, 4281–4286.
Seelig, A., & Seelig, J. (1974) *Biochemistry 13*, 4839–4845.
Shrake, A., & Rupley, J. A. (1973) *J. Mol. Biol. 79*, 351–372.
Tanford, C. (1974) *The Hydrophobic Effect: Formation of Micelles and Biological Membranes*, Wiley, New York.
Vickery, L. E. (1987) *Trends Biochem. Sci. 12*, 37–39.
Von Heijne, G. (1981a) *Eur. J. Biochem. 116*, 419–422.
Von Heijne, G. (1981b) *Eur. J. Biochem. 120*, 275–278.
Von Heijne, G. (1986a) *J. Mol. Biol. 189*, 239–242.
Von Heijne, G. (1986b) *EMBO J. 5*, 3021–3027.
Von Heijne, G., & Blomberg, C. (1979) *Eur. J. Biochem. 97*, 175–181.
Wallach, D. F. H., & Zahler, P. H. (1966) *Proc. Natl. Acad. Sci. U.S.A. 56*, 1552–1559.
Weinstein, J. N., Blumenthal, R., van Renswoude, J., Kempf, C., & Klausner, R. D. (1982) *J. Membr. Biol. 66*, 203–212.
White, S. H., Jacobs, R. E., & King, G. I. (1987) *Biophys. J. 52*, 663–665.
Wickner, W. T. (1988) *Biochemistry 27*, 1081–1086.
Wickner, W. T., & Lodish, H. F. (1985) *Science 230*, 400–407.
Woolfson, M. M. (1970) *An Introduction to X-ray Crystallography*, p 380, Cambridge University Press, Cambridge.
Worcester, D. L., & Franks, N. P. (1976) *J. Mol. Biol. 100*, 359–378.
Yeates, T. O., Komiya, H., Rees, D. C., Allen, J. P., & Feher, G. (1987) *Proc. Natl. Acad. Sci. U.S.A. 84*, 6438–6442.

μ-Conotoxin GIIIA, a Peptide Ligand for Muscle Sodium Channels: Chemical Synthesis, Radiolabeling, and Receptor Characterization†

Lourdes J. Cruz,‡,§ Gotfryd Kupryszewski,∥,⊥ Garth W. LeCheminant,‡ William R. Gray,‡ Baldomero M. Olivera,*,‡ and Jean Rivier∥

Clayton Foundation Laboratories for Peptide Biology, The Salk Institute, La Jolla, California 92037, Department of Biology, University of Utah, Salt Lake City, Utah 84112, and Department of Biochemistry and Marine Science Institute, University of the Philippines, Metro-Manila, Philippines

Received May 11, 1988; Revised Manuscript Received September 15, 1988

ABSTRACT: The peptide conotoxin GIIIA from *Conus geographus* L. venom, which specifically blocks sodium channels in muscle, has been synthesized by a solid-phase method. The three disulfide bridges were formed by air oxidation. After HPLC purification, the synthetic product was shown to be identical with the native conotoxin GIIIA from *Conus geographus*. A high specific activity, ^{125}I derivative of μ-conotoxin was prepared and used for binding assays to the Na channel from *Electrophorus* electric organ. Specific binding could be abolished by competition with tetrodotoxin. The radiolabeled toxin was specifically cross-linked to the Na channel. These studies demonstrate that μ-conotoxin GIIIA can be used to define the guanidinium toxin binding site and will be a useful ligand for understanding functionally important differences between Na channel subtypes.

The sodium channel is presently the best understood voltage-sensitive ion channel, both because of the detailed electrophysiology available and because of the wealth of biochemical data including complete sequence information from cloning experiments [for reviews, see Barchi (1988); Salkoff et al. (1987), Strichartz et al. (1987), Catterall (1986), and Agnew (1984)]. This remains the model system for understanding how changes in voltage across a membrane can result in a change in ion permeability. An important remaining goal is to identify the functionally important parts of the molecule. For example, it has long been known that the heterocyclic guanidinium toxins (tetrodotoxin and saxitoxin) bind at a site on the channel and prevent sodium permeation; this well-known toxin binding site has yet to be localized within the

† This work was supported by NIH Grants GM22737 (to B.M.O.), GM34913 (to W.R.G.), and AM26741 (to J.R.).
* To whom all correspondence should be addressed.
‡ University of Utah.
§ University of the Philippines.
∥ The Salk Institute.
⊥ Visiting scientist from the Institute of Chemistry, University of Gdansk, 80-952 Gdansk, Poland.

0006-2960/89/0428-3437$01.50/0